The Influence Of Sea Surface Temperature Anomalies On Low-Frequency Variability Of The North Atlantic Oscillation

Julia V. Manganello
and
J. Shukla

Center for Ocean-Land-Atmosphere Studies
Institute of Global Environment and Society
4041 Powder Mill Road, #302
Calverton, Maryland 20705
email: julia@cola.iges.org

Abstract

The influence of sea surface temperature (SST) anomalies on multi-year persistence of the North Atlantic Oscillation (NAO) during the second half of the 20th century is investigated using the Center for Ocean-Land-Atmosphere Studies (COLA) Atmospheric GCM (AGCM) with an emphasis on isolating the geographic location of the SST anomalies that produce this influence. In contrast to many studies on this subject, modeling work in this study is focused on calculating atmospheric response to the SST anomalies averaged over 1988-1995 (1961-1968) corresponding to the empirically derived time period of strong persistence of the positive (negative) phase of the decadal NAO. Atmospheric response to this forcing is estimated by averaging the modeled atmospheric behavior over the record of simulation and comparing it to the control simulation.

Response of the COLA AGCM to the global 1988-1995 average SST anomalies shows a statistically significant large-scale pattern in the North Atlantic characteristic of the positive phase of the NAO, though weaker in magnitude compared to the observations. Forcing with the global 1961-1968 average SST anomalies generates a negative NAO, however, barely significant and with less realistic structure compared to the 1988-1995 forcing. Additional analysis and linearity test reveal that over the centers of the NAO non-linear component of the forced response is quite important and acts to enhance the positive NAO signal.

Forcing of the COLA AGCM with the 1988-1995 average SST anomalies restricted to the Tropical Indo-Pacific region produces a positive NAO quite similar to the model response under the global 1988-1995 forcing. Analysis of multiple fields strongly suggests that anomalous boundary forcing leading to the persistence of the NAO in its positive polarity during 1988-1995 comes predominantly from the Tropics of the Indian and Pacific Oceans. 200-hPa geopotential height response in these two experiments shows a positive anomaly over the southern center of the NAO embedded in the Rossby wave trains propagating from the western and eastern tropical Pacific.

SST forcing confined to the North Atlantic region does not generate a response statistically different from the control simulation. Results from the North Atlantic experiment suggest that SST forcing is confined primarily to the equatorial region, and is not strong enough to significantly affect the phase of the decadal NAO.

1. Introduction

The North Atlantic Oscillation (NAO) represents a seesaw in the sea level pressure (SLP) with anomalies of opposite polarity located around the centers of the Icelandic Low and the Azores High. It is a very robust phenomenon, present on a wide range of time scales, and is easily identifiable in SLP or geopotential height data using various analysis techniques. The NAO is most pronounced during winter months when it accounts for more than one-third of the total variance of the SLP field over the North Atlantic region. To quantify the strength of the NAO and its effect on other climate variables NAO Index is often defined as a normalized winter mean SLP difference between a station near Azores High and a station near Icelandic Low.

The NAO has a strong influence on the climate variability in the Atlantic, European and American regions. Oscillations in the north-south SLP gradient, that it essentially represents, directly translate into changes of the surface westerlies across North Atlantic into Europe. Differences between winters of strong positive NAO and strong negative NAO include strengthening of westerlies onto Europe by more than 8 m/s, increased southerly flow over the eastern U.S. and increased northerly flow across western Greenland and the Mediterranean (Hurrell, 1995). The associated surface temperature changes due to thermal advection show cooling over the northwest Atlantic and northern Africa and warming over the southeast U.S. and from northern Europe across much of Eurasia. Fluctuations in the atmospheric flow associated with the NAO affect the transport and the convergence of atmospheric moisture causing changes in the regional precipitation patterns. During strong positive phase of the NAO the axis of maximum moisture transport shifts from west-to-east direction to more southwest-to-

northeast orientation across the Atlantic and extends much farther to the north and east onto the northern Europe (Hurrell, 1995). As a result, drier conditions occur over the central and southern Europe, Mediterranean and over much of Greenland with opposite changes taking place from Iceland to Scandinavia.

NAO fluctuations occur on multiple time scales ranging from intraseasonal to interdecadal. Analysis of the NAO Index defined as a difference of normalized winter mean (December-March average) SLP anomalies between Ponta Delgada, Azores, and Stykkisholmur, Iceland, from 1865 to 1997 (see Fig. 1a), revealed maximum variability at biennial and 6-10 year time scales. (Fig. 1b displays the leading North Atlantic EOF of December-March average SLP anomalies based on NCEP data for 1949-1998. The dipole pattern, present in Fig. 1b, often represents the spatial structure of the NAO.) It was found that much of the variance at biennial periods came from the early part of the record, and variability at interannual to decadal time scales became most pronounced during the latter half of the 20th century (see Fig. 2).

Much of the atmospheric circulation variability in the form of the NAO could arise from processes internal to the atmosphere. However, certain features of the observed NAO, like its phase and recent strong trend toward the positive polarity, may be influenced by surface, stratospheric or even anthropogenic processes. The assumption that current variability of the NAO is generated internally in the atmosphere remains a valid null hypothesis.

A number of recent modeling studies such as Rodwell et al. (1999), Mehta et al. (2000) have produced strong evidence in support of the hypothesis that oceanic forcing is responsible for decadal variability of the NAO during the second half of the 20th century.

In both studies an ensemble of simulations was generated where in each simulation an atmospheric GCM (AGCM) was forced by the observed record of sea surface temperatures (SSTs) and sea ice but was started from different initial atmospheric conditions. Boundary forced component of the variability was estimated by performing ensemble averaging. It was determined that low-frequency variability of the NAO forced by the ocean was quite similar to the observed, as was indicated by high degree of correlation between the low-frequency components of the observed and simulated ensemble-average NAO Indices. Relationship of the decadal NAO with surface temperature and precipitation was also captured quite well. There is no clear consensus at the moment, however, as to what area of the global ocean could be responsible for the observed decadal variability of the NAO. Modeling studies like the ones described above point to quite different regions of the global ocean, e.g. North Atlantic, tropical Atlantic, tropical Pacific, where SST changes are believed to force the phase shifts in the NAO on multi-year time scales.

One of the main goals of this study was to better identify the geographic origin of the oceanic forcing that is believed to drive decadal variability of the NAO. Compared to the majority of modeling studies on this subject, a more simplified experimental design was chosen in this work. The emphasis was on creating an appropriate boundary forcing, where SST anomalies, either global or confined to selected geographical regions, were averaged over the time periods characterized by strong persistence of either positive or negative phase of the NAO and added to the SST climatology. Atmospheric response to this averaged SST forcing was estimated by averaging the modeled atmospheric behavior over the whole record of simulation and comparing it to the control simulation

where the same AGCM was forced by the SST climatology. This experimental design has a number of advantages: (1) it requires much less computer resources to complete a single experiment and therefore allows to perform a number of "SST Anomaly" simulations to explore in more detail the geographic origin of the oceanic forcing of the NAO; (2) such an idealization of the boundary forcing is expected to produce some average response by the atmosphere, compared to the forcing by the historic record of SSTs and sea ice, which would potentially simplify interpretation of the physical processes involved in communicating boundary change to the atmospheric flow (of course, this is valid to the extent that the atmospheric response to the SST anomalies is linear); 3) spurious low-frequency variability that could interfere with the boundary forced signal is considerably reduced in the model forced by the same seasonally varying SSTs every year of the model simulation compared to the time-varying (annually and seasonally) SST forcing.

Experimental design is described in more detail in Section 2. Model experiments and main experimental results are presented in Section 3 followed by discussion of model results in Section 4, summary and conclusions in Section 5 and the list of references.

2. Experimental design

To study the oceanic influence on the NAO a series of "SST Anomaly" experiments were carried out and each compared to the "Climatological SST" experiment, which played a role of the control simulation. The main difference between these model simulations was the SST forcing. In the "SST Anomaly" experiments AGCM was forced by carefully constructed SST anomalies, averaged over the time

period when the NAO exhibited strong multi-year persistence of either positive or negative phase, and added to the SST monthly climatology. (For simplicity, sea ice was assigned its climatological monthly values.) In the "Climatological SST" experiment both SSTs and sea ice retained their climatological values.

Time averaging of the global SST anomalies was performed based on quantitative assessment of the NAO strength and persistence and also based on confidence in the observed SST record. For this purpose the NAO Index defined as a difference of normalized winter mean (December-March average) SLP anomalies between Ponta Delgada, Azores and Stykkisholmur, Iceland for 1865-1997 was low-pass filtered (LPF) with cut-off periods at 6, 10 and 26 years corresponding to the minima in the NAO Fourier Spectrum. (The choice of Ponta Delgada station in favor of Lisbon was dictated by the availability of data and was insignificant since according to Hurrell and van Loon (1997) the subtropical node of the NAO during northern winter is well captured either by Lisbon or Ponta Delgada). The resulting LPF NAO Index time series are shown in Fig. 3. The dashed lines in Fig. 3 represent the values of average plus (minus) standard deviation of the corresponding LPF NAO Index time series. (The solid lines represent the average of each time series, which in all three cases is practically zero). The periods of strong persistence of the decadal NAO anomalies were then defined as time intervals when the LPF NAO Index maintained one sign and its absolute value was equal or exceeded half of the standard deviation. Based on the above definition the appropriate periods for averaging of SST anomalies are 1988-1995, 1983-1996 or 1978-1997 (positive phase of the NAO) and 1961-1968, 1956-1969 or 1954-1973 (negative phase of the NAO), which are shown by filled circles in Fig. 3. The duration of each period of

strong persistence of the positive and negative phase of the NAO was limited by the duration of the shortest period among the two to eliminate the difference in sampling errors. The choice was limited to the last fifty years when the SST data was considered most reliable. It was decided to limit the choice of averaging periods to 1988-1995 for the positive phase of NAO and 1961-1968 for the negative one since the variability of the NAO at timescales longer than 7 years could be of the oceanic origin according to the majority of recent studies on the NAO. Annual cycle of SST anomalies averaged over the periods of 1988-1995 and 1961-1968 is shown in Figs. 4 and 5 respectively.

The goal of the experimental design was to construct boundary forcing most related to the persistence of the NAO in a certain phase and at the same time simplified enough to allow repeating the experiment multiple times with this SST forcing restricted to particular regions of the global ocean. Therefore, natural compromise was to create SST forcing constant in time but seasonally varying. It was also assumed that there was sufficient linearity in the response of the NAO to the SST forcing, at least within the chosen time periods when the NAO was very persistent in one phase, so that forcing of the NAO by time-averaged SSTs would be representative of the average effect of time varying SSTs on the NAO (see Section 4.1 for more details). Therefore, simple time averaging was the final choice. Period of 1988-1995 contains a strong La Niña, a strong El Niño and two El Niño events of average strength. A question could arise, whether it is an accumulated effect of these ENSO events that influences the phase of the NAO. First of all, it cannot be ruled out that it is the time-averaged ENSO that affects the NAO. There is no consensus at the moment regarding the effect of ENSO on the NAO. Observational study of Huang et al. (1998) showed that there is a connection between

ENSO and the NAO only during 70% of strong warm events, and the NAO in these cases is predominantly in its positive phase. On the other hand, modeling studies using AGCM (Gr_tzner et al. 2000) and Coupled GCM (Roeckner et al. 1996) show connection between warm ENSO events and the negative phase of the NAO. However, it was confirmed under more careful examination of monthly SSTs during individual years in the period of 1988-1995 compared to the 1988-1995 averaged SSTs that ENSO signal was significantly reduced, if not practically eliminated, as a result of averaging. The same was true for the 1961-1968 averaging period. Therefore, it is believed that ENSO would not significantly affect the model response.

3. Model experiments

Experimental work in this study was performed with the Center for Ocean-Land-Atmosphere Studies (COLA) AGCM. It is a global spectral model at T42 horizontal resolution (triangular truncation with 42 being the largest wave number resolved) with 18 sigma levels in the vertical. Schneider (2002) further describes numerical treatment of the dynamics and the parameterization of the sub-grid physical processes of COLA AGCM. Boundary forcing used in the model experiments was derived from Hadley Centre monthly sea ice and SST data for the period of 1948-1998 preprocessed for T42 resolution. In each experiment COLA AGCM was initialized with the atmospheric state on November 10, 1948, and was integrated in most cases for 50 years.

3.1) Global 1988-1995 SST Anomaly Experiment

"Global 1988-1995 SST Anomaly" experiment (8895 GLOBAL hereafter) was conducted to determine whether the oceanic forcing could be responsible for persistence

of the positive phase of the NAO on decadal timescales. Boundary forcing included monthly sea ice fraction climatology and monthly SST distributions, where global SST anomalies averaged over 1988-1995 corresponding to the period of strong persistence of the positive phase of the NAO were added to the SST climatology.

Fig. 6b shows the difference between December-March (DJFM) 500-hPa geopotential height field from this experiment, averaged over 50 years of model integration, and the equivalent one from the "Climatological SST" experiment (CLIM hereafter). Fig. 6a shows the difference between DJFM mean 500-hPa geopotential height from National Centers for Environmental Prediction-National Center for Atmospheric Research (NCEP-NCAR) reanalysis data (NCEP hereafter) averaged over 1988-1995 and 1949-1998 included for comparison with Fig. 6b. All the major features on the difference maps are statistically significant at 95% confidence level according to the pointwise Student's t-test, as shown in Figs. 6e and 6f. (According to the current experimental design any model simulated long-term mean, or time average over the whole record of model integration, is equivalent to the boundary forced component of the climate variable in question, provided this record is long enough to effectively average out atmospheric noise.) Fig. 6 shows some important similarities between the model results and observational data: both difference maps (Figs 6a and 6b) display dipole pattern in the North Atlantic corresponding to the positive phase of the NAO, though the model NAO is slightly shifted to the northwest and its northern center is weaker compared to the observations. The largest differences amount to a large trough over the North Pacific and no signal over Europe in the model results. NCEP difference map is primarily zonal in character with practically no signal in the North Pacific. These

differences will be further addressed in Section 4.2. The above results to a large degree are also applicable to the DJFM mean of Sea Level Pressure (SLP) (Figs.7a and 7b). All major features in the SLP difference maps are significant at the 95% confidence level as well, as shown in Figs. 7e and 7f.

Table 1 summarizes basic statistics of the NAO indices from different experiments and observational data. (SLP anomalies of these station-based NAO indices were averaged approximately over the locations of Ponta Delgada, Azores and Stykkisholmur, Iceland). Average value of the NAO Index from the CLIM experiment, calculated over 50 years of simulation, is zero according to the NAO Index definition. When 50-year average SLP from the CLIM experiment is used to calculate SLP anomalies from the 8895 GLOBAL simulation, average value of the NAO Index becomes 1.32. According to the current experimental design this signifies a change toward the positive phase of the NAO when model atmosphere is forced by the global SST anomalies averaged over 1988-1995. Application of the two-tailed Student's t-test shows that this change is statistically significant at 99% confidence level. Moreover, as Table 1 indicates, 1.32 is higher than the standard deviation of LPF≥6 Station NAO Index for 1865-1997, which is 1.13. This means that the positive change in the NAO in the 8895 GLOBAL experiment is strong enough to fall under the empirically derived definition of strong NAO activity. However, this positive change is not as high as the average of the LPF≥6 Station NAO Index over 1988-1995, which is 1.76.

Constant in time boundary forcing, as implemented in the idealized experiments, generates forced response that is constant in time, at least on interannual and longer timescales. For this reason, standard deviations of the NAO Indices from the idealized

experiments represent unprocessed, unfiltered noise, whereas standard deviations of the station and NCEP NAO Indices, as shown in Table 1, are computed for LPF data. Therefore, there appears to be a difference in standard deviations between the NAO Indices from the idealized experiments and observations. In fact, standard deviation of the unfiltered NAO Index from NCEP reanalysis for 1949-1998 is 1.87, which is comparable to the standard deviation of the NAO Index from 8895 GLOBAL experiment (1.81). Average standard deviation of unfiltered NAO Indices from 10-member ensemble simulation with COLA AGCM of the same T42 resolution forced by the observed record of SSTs and sea ice during 1948-1998 and performed as part of the Climate of the 20th Century Project (C20C) has also a similar value (1.75).

Nevertheless, based on the calculation of the NAO Indices, free variances do appear to be rather large. To estimate statistical significance of the forced response pointwise Student's *t*-test was appled to 500-hPa geopotential height data (Fig. 6f) and SLP data (Fig. 7f), and showed that the forced response was particularly strong over the southern center of the NAO where it was comparible to the observations in magnitude. One of the disadvantages of the Student's *t*-test is that given large enough sample size it could yield statistical significance even when the signal is too weak to be physically significant. To estimate the degree of separation between the forced and the unforced response pointwise (0.5,p)-recurrence test was performed on the same SLP field (Fig. 8). (For more information on this test see von Storch and Zwiers (1999)). It could be seen that the forced response is distinct only over the portion of the southern center of the NAO. In the "Tropical Indo-Pacific 1988-1995 SST Anomaly" experiment (8895 TropIP) (see Section 3.3) it could be marginally field significant. These results agree with a

separate analysis of SLP variance in the COLA C20C experiment where it was determined that during 1988-1995 signal-to-noise ratio over the southern center of the NAO increased as high as 65%-72% depending on the geographical averaging of the time series.

To examine the oceanic forcing of the atmosphere monthly means of the total precipitation, which is a good estimate of the vertically integrated latent heat release, were also calculated (Fig. 9). Large area of increased rainfall with decreased precipitation to the south is present in the equatorial Indian and western Pacific Oceans during late summer to winter months. In the central and eastern equatorial Pacific regions of anomalous precipitation are smaller in scale but appear to correspond to the surface heat fluxes both in location and time (not shown). Annual cycle of the 28-degree isotherm in the SST distribution used in CLIM, 8895 GLOBAL and "Global 1961-1968 SST Anomaly" experiments (6168 GLOBAL hereafter) (Fig. 10) could shed some more light on the origin of the anomalous boundary forcing in the model experiments. 28-degree isotherm is generally used as a proxy for the geographical extent of the warm pool and its location could indicate the onset of active atmospheric convection. As Fig. 10 indicates, only in 8895 GLOBAL experiment 28-degree isotherm extends through the whole equatorial Pacific (only in summer and fall), thus "closing the gap" between the western and eastern Pacific. Accordingly, anomalous heat fluxes and rainfall are observed in about the same months and in the same regions. In the western Pacific and Indian Oceans 28-degree contours from the 8895 GLOBAL and CLIM experiments closely follow each other, except during winter months when the largest discrepancies occur in the Indian Ocean. This observation points out that both western Pacific/Indian

Ocean and eastern Pacific could be the source of anomalous boundary forcing generating the model response described in this section.

Analysis of observed precipitation does not yield entirely the same results as analysis of model data. Fig. 11 shows difference maps of monthly climatology of total precipitation comparing data from the Climate Prediction Center Merged Analysis of Precipitation (CMAP hereafter) by Xie and Arkin averaged over 1988-1995 and 1979-2001 (with strong ENSO years of 1982/83, 1986/87, 1988/89, 1991/92, 1997/98 and 1999/2000 excluded). The best agreement between model results in Fig. 9 and observational data in Fig. 11 is achieved during January and February, though the region of negative precipitation anomalies is a lot larger in observations. During other months decreased rainfall is observed over most of the equatorial Indian Ocean and extreme western Pacific. There are no precipitation anomalies over the eastern Pacific. In addition, application of Student's t-test revealed that none of the anomalies in Fig. 11 are statistically significant.

3.2) Global 1961-1968 SST Anomaly Experiment

6168 GLOBAL experiment was conducted to determine whether the oceanic forcing could be responsible for persistence of the negative phase of the NAO on decadal timescales. Boundary forcing included monthly sea ice fraction climatology and monthly SST distributions, where global SST anomalies averaged over 1961-1968 corresponding to the period of strong persistence of the negative phase of the NAO were added to the SST climatology.

Fig. 12 shows DJFM mean 500-hPa geopotential height field from this experiment, averaged over 50 years of model integration, and the difference between this

mean and the equivalent one from the CLIM experiment (Fig. 12b). Fig. 12 also shows the difference between the NCEP DJFM mean 500-hPa geopotential height averaged over 1961-1968 and 1949-1998. There are some significant differences between model results and observational data: dipole pattern in the North Atlantic in the model data is of opposite polarity compared to the observations and corresponds to the positive phase of the NAO. It is also much weaker and has a very different geographical position of its southern center. In addition, all large-scale features both in the model and observations are much weaker in magnitude compared to the 1988-1995 period and are barely significant at 95% confidence level according to the pointwise Student's t-test (not shown).

Considering the fact that the negative phase of the NAO when averaged over 1961-1968 could represent a weak signal, it is possible that 50 years of integration is not sufficient to filter out the boundary forced signal from the atmospheric noise. With this in mind COLA AGCM was integrated for additional 50 years, making the total integration time equal to 100 years. Results shown in Fig. 12 were recomputed using 100 years of integration in the 6168 GLOBAL experiment framework. Model dipole pattern in the North Atlantic still corresponds to the positive phase of the NAO but is of weaker magnitude compared to the result when only 50 years of data are analyzed (not shown). Integration of the COLA AGCM for additional 50 years, making the total integration time equal to 150 years, did not lead to any significant changes, indicating that the structure in Fig. 12b does indeed correspond to the boundary forced signal.

It appears from the analysis of model data that the model failed at least to produce adequate surface forcing in order to generate strong enough response in the atmosphere.

Comparison of NCEP monthly means of the surface heat flux (sum of latent, sensible and upward LW fluxes at the surface) for the period of 1961-1968 and for the period of 1988-1995 revealed important similarities. During the months of May to about December within 1961-1968 and 1988-1995 anomalous surface heat fluxes of opposite sign are observed over quite large area in the eastern tropical Pacific (not shown). (These surface heat fluxes are statistically significant during both periods of analysis). Change of sign of the anomalous surface heat fluxes also takes place in the tropical Indian and western Pacific Oceans during winter months but over much smaller geographical area. Contrary to the observations, anomalous surface heat fluxes of opposite sign and the same geographical location are not found in the 6168 GLOBAL experiment compared to the 8895 GLOBAL experiment. Moreover, 6168 GLOBAL simulation practically did not produce any significantly strong large-scale surface heat fluxes with respect to the CLIM simulation (not shown). Further analysis of the results of this experiment is deferred to Sections 4.1 and 4.2.

The above-described results seem to correspond to the main findings of Straus and Shukla (2002) who studied mid-latitude response to the ENSO forcing. They discovered that response to the cold SST anomalies is not robust, is harder to separate from the internal variability and there is a highly nonlinear relationship between cold SST anomalies and tropical heating anomalies. On the other hand, response to the warm anomalies has a clear pattern and there is a linear relationship between positive SST anomalies and corresponding tropical heating.

3.3) Tropical Indo-Pacific 1988-1995 SST Anomaly Experiment

Analysis of the 8895 GLOBAL experiment indicated that forcing of the COLA AGCM by global SST anomalies averaged over 1988-1995 lead to a positive change in the model NAO. To further examine the oceanic influence on the multi-year persistence of the NAO, the following experiment (8895 TropIP hereafter) was conducted, where 1988-1995 average SST anomalies were retained only over Tropical Indo-Pacific region (see Fig. 13, top panel) and SST climatology was used elsewhere. Though earlier studies focused mostly on the link between the ENSO and the NAO and produced contradictory results, recent study by Hoerling et al. (2001) showed a link between North Atlantic climate change since 1950 and a progressive warming of tropical SSTs, especially over the Indian and Pacific Oceans, which prompted to single out this region to examine its effect on the NAO in this study.

Comparison of the DJFM 500-hPa geopotential height response to the Tropical Indo-Pacific SST forcing and global SST forcing averaged over 1988-1995 reveals strong similarities (see Figs. 6b and 6c). Most importantly, the hemispheric-scale structures of the 500-hPa geopotential height anomalies in these two experiments are remarkably similar. Largest differences are weaker northern center of the NAO and stronger signal in the North Pacific in the 8895 TropIP experiment. (Large-scale features in the difference map in Fig.6c are also statistically significant, as shown in Fig. 6g). The above results to a large degree are also applicable to the DJFM mean of SLP (Fig. 7). All major features in the SLP difference map (Fig. 7c) are significant at the 95% confidence level as well (Fig. 7g).

To quantify positive change in the NAO, as seen in Fig. 7c, station-based NAO Index was calculated with the long-term mean of SLP taken from the CLIM experiment

to calculate SLP anomalies. As is shown in Table 1, the average value of the NAO Index from the 8895 TropIP experiment is as high as 1.21 and the standard deviation is 1.62. Based on these parameters, this positive change is not statistically different from the positive change of the NAO Index in the 8895 GLOBAL experiment. This would mean that SST forcing from the Tropical Indo-Pacific region is strong enough to generate appropriate change towards positive polarity in the model NAO characteristic of the COLA AGCM under the current experimental design.

Analysis of monthly means of total precipitation, as expected, shows little difference in the tropical regions of the Indian and Pacific Oceans compared to the 8895 GLOBAL simulation. Since the largest anomalies in total precipitation occur in the tropics (see Fig. 9) the largest differences in precipitation between 8895 GLOBAL and 8895 TropIP experiments are confined to the tropical Atlantic (not shown), which, as it turns out, is not of major consequence for the change in the strength of the NAO.

Based on the results presented above, it is possible to conclude that the change towards the positive polarity in the NAO during 1988-1995 is primarily forced from the tropical regions of the Pacific and Indian Oceans. Further discussion on the mechanisms by which tropical forcing could affect the phase of the NAO is deferred to Section 4.4.

3.4) North Atlantic 1988-1995 SST Anomaly Experiment

To examine the local effect of SSTs on the multi-year persistence of the NAO rather than the remote effect that was studied in the 8895 TropIP simulation, "North Atlantic 1988-1995 SST Anomaly" experiment (8895 NAtl hereafter) was conducted. In this experiment 1988-1995 average SST anomalies were retained only over the North

Atlantic region (see Fig. 13, bottom panel, for exact geographical extent of the anomalies) and SST climatology was used elsewhere.

As seen in Fig. 6d, DJFM 500-hPa geopotential height response in the North Atlantic is also in the form of a dipole pattern resembling the positive phase of the NAO. However, compared to the results of the 8895 TropIP experiment, the southern center of the NAO has much weaker magnitude and, based on statistical significance calculations, geopotential height change over the southern center is insignificant altogether (Fig. 6h). The northern center is somewhat stronger but is shifted further to the west. Positive change in the NAO, though of weaker magnitude, is also evident in the DJFM SLP response shown in Fig. 7d. This change is not statistically significant at all (Figs. 7h and 8d), which is a drastically different outcome compared to the results of the 8895 GLOBAL and 8895 TropIP experiments. It is noteworthy that over the North Pacific both 500-hPa geopotential height and SLP develop a high in response to the North Atlantic SST anomalies, where there is a low when either global or Tropical Indo-Pacific SST anomalies are used.

Analysis of DJFM SLP variability in the North Atlantic reveals that NAO fluctuations are present in this experiment as well and represent a substantial part of the total variability. However, given the average value of the NAO Index equal to 0.66 and its standard deviation of 1.78 (see Table 1), the mean value of these coherent fluctuations is apparently too weak and the variability too high to make them statistically different from the NAO fluctuations characteristic of the CLIM experiment. In summary, compared to the SST forcing from the Tropical Indo-Pacific region, North Atlantic SST anomalies averaged over 1988-1995 generate NAO-like atmospheric variability but fail

to produce the significant positive change in the long-term mean NAO, as present in the observations.

Analysis of surface diabatic heating and precipitation also shows substantial differences with respect to the 8895 GLOBAL and 8895 TropIP experiments. The only large-scale statistically significant surface heat flux anomalies present in this experiment are observed in the extreme eastern equatorial Pacific during months of July through September and have opposite sign compared to both 8895 GLOBAL and 8895 TropIP experiments (not shown). In correspondence with these heat flux anomalies large-scale precipitation anomalies are also present in the same region during the same months. During late fall and winter the largest precipitation response is observed in the equatorial Atlantic (not shown). Though these precipitation anomalies are statistically significant, they are weaker in magnitude and smaller in scale compared to the precipitation anomalies from the 8895 GLOBAL and 8895 TropIP experiments both in equatorial Pacific and Atlantic.

4. Discussion of model results

4.1) Comparison with observations and COLA AGCM ensemble simulation

Figs. 14 and 15 compare results of the 8895 GLOBAL and 6168 GLOBAL simulations with NCEP data and with results of the COLA C20C 10-member ensemble simulation. The goal of this comparison is to determine to what extent model response to the SST forcing averaged over 1961-1968 and 1988-1995 is similar to the average response forced by realistic, time-varying SSTs during the same time periods, i.e. to what

extent the model response is linear, which would then determine whether Localized SST Anomaly experiments were justified.

The top panels of Fig. 14 shows 1988-1995 and 1961-1968 average NCEP DJFM 500-hPa geopotential height anomalies computed relative to the 1949-1998 climatology. Over the North Atlantic 1988-1995 average anomalies clearly show a pattern characteristic of a strong positive phase of the NAO and 1961-1968 average anomalies show respectively a negative NAO phase distribution, both also present in SLP data (top panel, Fig. 15). Middle panel of Fig. 14 shows an estimate of the boundary forced response in the C20C experiment during 1988-1995 and 1961-1968 given by corresponding time-average ensemble-average DJFM 500-hPa geopotential height anomalies calculated relative to the ensemble-average 1949-1998 observed SST integration and referred to as 8895 C20C - 4998 C20C and 6168 C20C – 4998 C20C respectively. First of all, the response is a lot weaker in magnitude compared to the observations. It does, however, correspond to the positive phase of the NAO for 1988-1995 average data and to the negative phase for 1961-1968 average data. 1961-1968 anomaly distribution is more realistic, whereas 1988-1995 anomalies are less localized over the centers of the NAO and appear more in the northeast-to-southwest, rather than north-south, direction. The same conclusions are applicable to the corresponding SLP data (middle panel, Fig. 15), with the exception of better north-south orientation of the NAO dipole in the 1988-1995 average. Bottom panel of Fig. 14 shows a boundary forced response in the 8895 GLOBAL and 6168 GLOBAL experiments computed with respect to the same ensemble-average 1949-1998 observed SST integration of the C20C experiment and referred to as 8895 GLOBAL – 4998 C20C and 6168 GLOBAL – 4998

C20C respectively. 500-hPa geopotential height anomalies from the 8895 GLOBAL experiment are stronger in magnitude and more realistic in spatial distribution compared to the corresponding C20C data. Anomalies from the 6168 GLOBAL experiment are similar in magnitude to the corresponding C20C anomalies but barely resemble the negative phase of the NAO. Corresponding SLP data (Fig. 15, bottom panel) also confirm these conclusions.

In overall, the 8895 GLOBAL experiment better simulates the positive phase of the NAO than the C20C experiment, which could be partly due to insufficient number of model realizations in the C20C experiment to effectively filter out boundary forced signal, as shown by Mehta et al. (2000). However, the model NAO from either experiment is still much weaker than its observational counterpart. In addition, based on statistical significance calculations (not shown), SLP anomalies over the northern center of the NAO are not statistically significant at 95% confidence level. Model response in the 6168 GLOBAL experiment has a weak projection onto the negative phase of the NAO compared to the observations and the corresponding C20C data. It must be noted that both 500-hPa geopotential height and SLP anomalies in the C20C experiment during 1961-1968 are statistically significant over much larger areas than the corresponding NCEP and 6168 GLOBAL anomalies. (In fact, these statistically significant NCEP anomalies have very limited geographic coverage and therefore might not be field significant (not shown)). Based on the above and considering data limitations, it can be concluded that time averaging of the SST forcing does generate a change in the NAO of the correct sign, though it is skewed towards the positive NAO polarity. This bias is essentially a non-linear part of the COLA AGCM response to the time-averaged SST

forcing versus time-varying SST forcing, and is more directly shown in Figs. 16 and 17. Based on statistical significance maps in these figures, this non-linear response is fortunately confined to the extreme western Atlantic and extreme eastern Atlantic (only for 1961-1968 averaging), away from the bulk of the NAO response in the model (see Figs. 14e and 14f, and also Fig. 6b). Based on the above it is possible to state that in the COLA AGCM the NAO response to the time averaging of the SST forcing within the chosen time periods is essentially linear.

To compare the boundary forcing, corresponding anomaly maps of total precipitation were computed (see Fig. 18). First, the top panel of Fig. 18 shows 1988-1995 and 1961-1968 average SST anomalies based on Hadley Centre monthly SST data and relative to the 1949-1998 climatology of the same dataset. It is obvious that 1988-1995 average SST anomalies are predominantly positive, whereas 1961-1968 average SST anomalies are mostly negative. Fig. 18c displays 1988-1995 average precipitation anomalies from the CMAP data of Xie and Arkin calculated relative to the 1979-2001 climatology with ENSO years excluded. Figs. 18e and 18g show respectively 1988-1995 average ensemble-average anomalies from the C20C data and 50-year average anomalies from the 8895 GLOBAL experiment, both computed with respect to the 1949-1998 ensemble-average long-term mean of the C20C experiment. The above three precipitation maps have the following features in common: 1) the largest anomalies are confined to the tropical regions of the Pacific ocean and are fairly similar in magnitude; 2) there is a large negative precipitation anomaly in the extreme Western Pacific with a large positive one to the east. Biggest differences between observations and experimental results are large precipitation anomalies present also in the Indian Ocean, Eastern

Equatorial Pacific and Equatorial Atlantic in the model data. Corresponding anomalies for the 1961-1968 time period are shown in Fig. 18f and 18h and to a large extent appear to be of opposite sign.

4.2) Comparison of climatologies from Climatological SST experiment and COLA AGCM ensemble simulation

To understand the differences between model results, as shown in Figs.14 and 15, where COLA AGCM response in the 8895 GLOBAL and 6168 GLOBAL experiments was demonstrated relative to the ensemble-average long-term means of the C20C experiment data, and results in Figs. 6, 7 and 12 where the same response was shown with respect to the long-term averages of the CLIM experiment, the above mentioned long-term means were examined in more detail. Thus Fig. 19 (top panel) displays the difference of ensemble-average 50-year average of DJFM total precipitation from C20C experiment data and DJFM total precipitation from the CLIM experiment data, averaged over 50 years of model integration. Fig. 19 (middle panel) shows corresponding results for 500-hPa geopotential height and Fig. 19 (bottom panel) assesses their statistical significance. Data was not detrended in Figs. 19a, 19c and 19e and was detrended respectively in Figs. 19b, 19d and 19f. It is worth reiterating that the main difference between C20C and CLIM experiments is the boundary forcing: in the former SSTs are annually varying, which means that *both annual and decadal variations* are preserved, and in the latter SSTs have their climatological mean values for each month averaged over the whole observational record. As a result, model response to this annually varying forcing is dominated by the years of *positive* SST anomalies and hence increased lower tropospheric heating in the tropics, as shown in Fig. 19a, which strongly resembles Figs. 18e and 18g. It is therefore not surprising that the corresponding 500-hPa geopotential

height response is dominated by the positive NAO pattern in the North Atlantic, as well as enhanced Aleutian Low (Fig. 19c). Negative SST anomalies can also lead to the negative NAO distribution, however, based on the results of the C20C experiment their effect is not as strong as the effect of the positive SST anomalies, at least on average over the chosen time period (1949-1998). It is noteworthy that detrending data and thus eliminating the linear effect of multi-decadal SST variability (climate change) quite significantly changes the resulting distribution: strong low over the North Pacific in the 500-hPa geopotential data practically disappears. However, projection on the positive NAO distribution in the North Atlantic still remains (see Fig. 19d).

Fig. 20 combines Figs. 14, 19, 6 and 12 and is presented primarily for illustration purposes to better summarize and explain the main results of this study. Fig. 12c shows 500-hPa geopotential height response from the 8895 GLOBAL experiment relative to the model climate forced by the annually varying SSTs (C20C experiment) described in detail in Section 4.1. Fig. 20e shows the difference between the C20C mean and the one forced by the SST climatology (CLIM experiment) and finally Fig. 20g shows the same response from the 8895 GLOBAL experiment but relative to the simulation forced by the SST climatology, which constitutes the main experimental result described in Section 3.1. Figs. 20d, 20f and 20h display the same data but for the 1961-1968 period. In essence, Fig. 20c depicts *decadal* NAO in its positive polarity relative to the *"realistic"* model climate since applied boundary forcing is decadal. Fig. 20e contains *both interannual and decadal* SST forced response, where at least in the North Pacific patterns are dominated by the interannual SST variability and in the North Atlantic the resultant pattern is also NAO in its positive polarity. Fig. 20g shows *decadal* NAO in its positive

polarity relative to the *"idealistic"* model climate and is effectively the sum of Figs. 20c and 20e. It is now more clear why NAO in Fig. 20g is so strongly positive: it is of the same sign in Figs. 20c and 20e. It is also clear why NAO in Fig. 20h is almost neutral or weakly positive: decadal NAO of negative polarity is weak in Fig. 20d and is of opposite sign to the NAO in Fig. 20f. In summary, when shown relative to the long-term means of the CLIM experiment model response from the 8895 GLOBAL and 6168 GLOBAL experiments is strongly skewed towards the NAO in the positive polarity primarily due to the absence of the significant non-linear component of the SST forced response in the reference climate.

4.3) Linearity test

Considering the apparent differences in the way model generates positive and negative change in the NAO in response to the boundary forcing, it appears necessary to assess the degree of linearity of the model response to the SST forcing. Model response to the SST anomaly is regarded as linear, if the change of sign of the SST anomaly leads to the response of the same magnitude and opposite sign compared to the long-term mean of the control experiment, i.e. experiment of zero SST anomaly. The assumption of linearity is embedded in the current experimental design. Indeed, if the NAO response to the SST anomaly forcing is non-linear, then the NAO forced by time-averaged SST anomalies could be quite different from the time-averaged NAO forced by historical record of the SST anomalies. This "requirement" of linearity is therefore a significant limitation of the current experimental design.

To perform a linearity test two additional model experiments were conducted with the asymmetric boundary forcing created as follows: 1961-1968 average global SST

anomalies corresponding to the negative phase of the decadal NAO were subtracted from the 1988-1995 average global SST anomalies corresponding to the positive phase of the decadal NAO; as a result, the geographical areas where SST anomalies differ the most between the two phases of the NAO got emphasized and the resulting anomalies were enhanced (not shown). This SST anomaly difference, taken with a positive sign, was used as a boundary forcing to simulate a positive change in the NAO in the experiment called " Global Positive SST Anomaly Experiment" (+SSTA hereafter). The same anomaly difference, taken with a negative sign, was used to simulate a negative change in the NAO, and the corresponding experiment was called "Global Negative SST Anomaly Experiment" (-SSTA hereafter).

Figs. 21a and 21b show DJFM 500-hPa geopotential height response to the SST forcing employed in the +SSTA and –SSTA simulations respectively, presented as a deviation of the 500-hPa geopotential height averaged over 50 years of model simulation from the corresponding average of the CLIM experiment. Also shown are the estimates of the non-linear and linear components of the forced response (Figs. 21c and 21d respectively). The size of non-linearity in this setup can be estimated by taking the *sum* of the responses to the SST anomalies of opposite polarity measured with respect to the long-term mean of the CLIM experiment, whereas the size of linearity can be estimated by taking the ***difference*** between the same quantities. After some simplifications the non-linear component of the forced response becomes equal to the difference between the average of the responses to the SST anomalies of opposite polarity and the long-term mean of the CLIM experiment: **(+SSTA – CLIM) + (-SSTA – CLIM) _ (+SSTA + -SSTA)/2.0 – CLIM**. Similarly, the linear component of the forced response becomes

equal to the differences of the responses to the SST anomalies of opposite polarity divided by two: **(+SSTA – CLIM) – (-SSTA – CLIM) _ (+SSTA – -SSTA)/2.0**. These are precisely the quantities shown in Figs. 21c and 21d. Though over much of North Atlantic linearity appears to dominate, this is not the case for the areas corresponding to the centers of the NAO. Based on the results of EOF analysis of North Atlantic SLP anomalies from the +SSTA and –SSTA experiments (not shown), northern center of the NAO is located over Iceland and eastern Greenland and the southern center covers large area over eastern Atlantic and south-western Europe. As Figs. 21c and 21d indicate, in these locations non-linear component of the forced response appears to be at least as important as the linear one. Moreover, non-linearity seems to be particularly critical when negative change in the NAO is generated. One way to look at this is to decompose the model response in the –SSTA simulation (Fig.21b) into the non-linear and linear components (Figs. 21c and 21d). In this situation non-linear and linear parts of the response act "out-of-phase", practically eliminating the negative NAO signal. (In the –SSTA experiment NAO change is equal to –0.3, which is statistically insignificant at 95% confidence level). On the other hand, in the case of the +SSTA experiment non-linearity acts "in sync" with linearity, enhancing the positive NAO signal. (Positive change in the NAO in the +SSTA experiment is equal to 1.16 being statistically significant at 95% confidence level). In addition, comparison of the –SSTA experiment with the 6168 GLOBAL one and the +SSTA with the 8895 GLOBAL shows that persistence of the positive phase of the NAO appears to be quite "robust" to the spatial structure and magnitude of the SST anomalies (spatial structure and magnitude of the

response in the +SSTA and 8895 GLOBAL experiments are very similar), whereas the opposite is true for the negative phase of the NAO.

This non-linearity in the geopotential height response to some extent could be originating from the non-linear relationship between the tropical heating and the underlying SST anomalies. Analysis of total precipitation demonstrates that non-linearity is confined to the western Pacific and Indian Ocean where atmospheric heating is the strongest and also to the eastern equatorial Pacific during months of October and November (not shown).

4.4) Rossby wave propagation

As was described in the previous sections, model NAOs forced by the SST anomalies in the Tropical Indo-Pacific region and the global SST anomalies appear to be remarkably similar. Results from the 8895 NAtl experiment also support the conclusion that positive change in the NAO, at least during 1988-1995, is forced non-locally, and to the most part the forcing comes from the tropical regions of the Indian and Pacific Oceans. It therefore seems appropriate to explore whether one of the well-known mechanisms, by which tropical convective heating can affect extratropical circulation, namely generation and propagation of Rossby wave trains, could be operating in these experiments.

Rossby wave motion is generated by upper-tropospheric divergence, which in turn is produced by local ascent due to convective heating in response to underlying SST anomalies. In the presence of westerly zonal flow long wavelength Rossby waves can propagate polewards as well as eastwards into the mid-latitudes. (To be precise, if, however, divergence occurs in the region of equatorial easterlies, advection of vorticity

by the divergent wind out of such a region can lead to Rossby wave generation in the westerly wind regions where their propagation is possible, as noted by Sardeshmukh and Hoskins (1988)). In the study of global response to the tropical heating using a primitive equation model Jin and Hoskins (1995) have determined that the propagating Rossby wave train is quasi-stationary in phase and has equivalent barotropic vertical structure.

Fig.22 shows zonally asymmetric part of January mean 200-hPa geopotential height response from the 8895 GLOBAL and 8895 TropIP experiments, presented as a deviation from the long-term mean of the CLIM experiment. (For midlatitude synoptic scale motions geopotential height is a good approximation for the streamfunction field). Fig. 23 shows corresponding maps for January mean 200-hPa meridional wind. (According to Jin and Hoskins (1995), upper-tropospheric meridional wind perturbation field provides much clearer picture of the origin and propagation of Rossby wave trains than e.g. streamfunction.) Anomalous 200-hPa geopotential height distribution in Fig. 22 is consistent with the 200-hPa meridional wind field in Fig. 23 with the exception that the latter shows strong wave activity in the extreme eastern equatorial Pacific, not seen in Fig.22. Patterns of both 200-hPa geopotential height and meridional wind response are very similar in the two experiments. From October to January strong wave activity is present in the eastern tropical Pacific (data for October to December is not shown). Starting November there is a measurable wave propagation from the eastern Pacific to the North Atlantic arching over Iceland to Central Russia. Location of the areas of positive and negative meridional wind anomalies in the North Atlantic corresponds to the increased westerlies across the region. Though most of the wave activity in December is concentrated in the Southern Hemisphere with wave trains emanating both from the

western and the eastern equatorial Pacific, January shows numerous wave trains propagating in both hemispheres. There is a large wave train across North America originating apparently in the western equatorial Pacific, and there is a very similar wave pattern over the North Atlantic as in November, though much stronger in magnitude. This wave pattern in the North Atlantic (Fig. 23) corresponds to the anomalous high in Fig. 22 which is colocated with the statistically significant 500-hPa geopotential height and SLP response in the 8895 GLOBAL and 8895 TropIP experiments (Figs. 6, 7 and 8). February (not shown) displays similar wave patterns to the ones in January, though equatorial wave activity is practically absent. In summary, November, January and February show arching Rossby wave trains over the North Atlantic corresponding to the enhanced westerlies in agreement with the positive change in the NAO. Since these wave trains are very similar in both 8895 GLOBAL and 8895 TropIP experiments, the anomalous stationary waves must be forced from the tropical Indian and/or Pacific Oceans. Equatorial wave patterns suggest that the eastern Pacific could be the main forcing region. To be able to conclude that propagation of Rossby wave trains into the North Atlantic due to forcing by tropical Pacific heating is the mechanism for persistence of the positive phase of the NAO, additional modeling studies need to be conducted.

It is encouraging that very similar wave patterns are present in the 200-hPa meridional wind data from the +SSTA experiment (not shown). There is an indication of anti-symmetric wave activity in the –SSTA experiment data, though wave trains over the North Atlantic are much weaker, except perhaps during months of February and March when they are clearly of opposite polarity.

5. Summary and conclusions

One of the main goals of this study was to better isolate the region where fluctuations in the SST are believed to drive the decadal variability of the NAO and to suggest the potential mechanism of forcing by repeating AGCM experiments with the SST forcing confined to selected parts of the global ocean. For this purpose experimental work was focused on generating atmospheric response to specifically constructed SST anomalies. These SST anomalies were averaged over 1988-1995 (1961-1968) corresponding to the time period of strong persistence of the positive (negative) phase of the decadal NAO, empirically derived based on the LPF NAO Index time series during 1865-1997. Atmospheric response to this averaged SST forcing was estimated by averaging the modeled atmospheric behavior over the whole record of simulation and comparing it to the control simulation. The control experiment was identical to the other AGCM experiments with the exception of the boundary forcing which was restricted to the SST and sea ice climatology derived from Hadley Centre monthly sea ice and SST data for the period of 1948-1998.

It was verified that response of the COLA AGCM to the 1988-1995 average global SST anomalies produced statistically significant large-scale pattern in the North Atlantic characteristic of the positive phase of the NAO, when compared to the control simulation, with quite realistic spatial structure. This response was particularly robust over the area corresponding to the southern center fo the NAO. Similarly, station-based model NAO Index displayed a large statistically significant positive change. However, this change was not as large as the 1988-1995 average LPF Station NAO Index, neither as the 1988-1995 average LPF station-based NCEP NAO Index, which would imply that

SST anomaly forcing used in the experiment could potentially account for only a fraction of the NAO persistence during this time period. Analysis of model surface heat flux and precipitation data suggested that both equatorial western Pacific/Indian Ocean and equatorial eastern Pacific could be the source of anomalous boundary forcing generating the positive change in the NAO. While the observations do show the largest precipitation anomalies during 1988-1995 in the equatorial western Pacific, there are no anomalies in the eastern Pacific. 1988-1995 average SST field in Fig. 4 that is used to force the positive change in the NAO is similar to the warming trend of the tropical Indian and Pacific SSTs (see Fig. 1 and Fig. 2 of Hoerling et al. 2001), and in fact could be responsible for the NAO persistence in the positive phase during this time period. To confirm or rule out the role of this warming trend additional experiments would need to be performed where it would be necessary to detrend SSTs before averaging or use scaled warming trend pattern to force the NAO.

In contrast with the previous experiment, forcing of the COLA AGCM with the 1961-1968 global SST anomalies did not produce the model response characteristic of the negative phase of the NAO. In fact, it produced a weak and barely significant positive change in the NAO with rather different spatial structure. Integration of the model for an additional 100 years to better filter out the boundary forced signal did not alter the results significantly. However, analysis of this model response relative to the ensemble-average long-term means of the C20C experiment, rather than the long-term means of the control simulation, produced quite different results. In this case it revealed statistically significant large-scale pattern in the North Atlantic that had a projection onto the negative phase of the NAO, though weak compared to the observations. However, model

response to the 1988-1995 average global SST anomalies preserved the pattern characteristic of the positive phase of the NAO. This pattern was still statistically significant but weaker in magnitude than the one relative to the long-term means of the control simulation, and on a hemispheric scale it was more similar to the observations. In terms of the boundary forcing, total precipitation anomalies in case of 1988-1995 forcing exhibited strong similarities with the observations. Though no observational counterpart was established for the case of 1961-1968 forcing, total precipitation anomalies in this experiment were to a large extent of opposite sign.

Analysis of the ensemble-average long-term means from the C20C experiment and the long-term averages of the control simulation confirmed that for the purpose of comparison with the observations it was more appropriate to compute model response relative to the ensemble-average long-term means of the C20C experiment. It was determined that when shown relative to the long-term means of the control simulation model response was strongly skewed in the North Atlantic towards the NAO in the positive polarity due to the absence of the significant non-linear component of the SST forced response in this reference climate. Since the boundary forcing in the C20C experiment was represented by *annually* varying SSTs, rather than *perpetual* SSTs averaged over the whole observational record as in the control simulation, due to non-linearity model response in this experiment was dominated by the years of positive SSTs and hence increased lower tropospheric heating which translated into the dominance of the positive NAO pattern in the North Atlantic. Detrending data did not eliminate this positive NAO bias. However, comparison of modeling results to the long-term averages

of the control simulation is still necessary in order to implement and analyze Regional SST Anomaly experiments.

In light of such strong non-linearities it appeared necessary to estimate directly the degree of linearity of the model response to the SST forcing. The linearity test was performed using two additional COLA AGCM experiments that employed global anti-symmetric SST anomaly forcing. It clearly showed that over the regions corresponding to the centers of the NAO non-linear component of the forced response was at least as important as the linear one, though over much of the North Atlantic linearity appeared to dominate. Moreover, non-linearity seemed to be particularly critical when negative change in the NAO was generated. In this situation non-linear and linear parts of the response acted "out-of-phase", practically eliminating the negative NAO signal, whereas in the case of the positive change non-linearity acted "in sync" with linearity, enhancing the signal. Analysis of the precipitation response revealed that non-linearity was primarily confined to the equatorial Pacific and Indian Oceans.

Analysis described in Section 4.1 confirmed, however, that model response to the SSTs within the time periods of 1988-1995 and 1961-1968 was fairly linear: time averaging of the SSTs within these periods generated change in the NAO of the correct sign, however, this change was somewhat skewed towards the positive NAO polarity. (This bias was essentially a non-linear part of the COLA AGCM response to the time-averaged SST forcing versus time-varying SST forcing, and based on statistical significance calculations it was confined to the extreme western Atlantic and extreme eastern Atlantic (only for 1961-1968 averaging), away from the bulk of the NAO response in the model.) This linearity was likely due to rather weak interannual

variability within these time periods and persistence of the decadal signal in one particular phase in accordance with the criteria used to select these time periods. The above conclusion thus justified implementation of Regional SST Anomaly experiments within the current experimental design.

To examine the effect of boundary forcing originiating in the tropical regions of the Pacific and Indian Oceans, COLA AGCM experiment was repeated with the anomalous SST forcing restricted to the Tropical Indo-Pacific region as specified in Fig 13a. Analysis showed that the hemispheric-scale patterns in the 500-hPa geopotential height and SLP anomaly fields were remarkably similar to the corresponding patterns in the 8895 GLOBAL experiment. North Atlantic variability showed substantial similarities as well: the leading EOF also represented NAO dipole with almost identical structure and station-based NAO Index also revealed a positive change. According to the Student's t-test this change was not statistically different from the positive change in the NAO Index in the 8895 GLOBAL experiment. The above results strongly suggest that anomalous boundary forcing leading to the persistence of the NAO in its positive polarity at least during 1988-1995 comes predominantly from the tropical regions of the Indian and Pacific Oceans. Analysis of the 200-hPa geopotential height and meridional wind response in these two experiments showed Rossby wave trains propagating from the eastern Pacific to the North Atlantic arching over Iceland to Central Russia during the months of November, January and February. Rossby wave trains originating from the western Pacific and arching over the North Pacific could also be clearly observed during January and February. Location of the areas of geopotential height and meridional wind anomalies in the North Atlantic corresponded to the increased westerlies across the

region in agreement with the positive change in the NAO, primarily due to positive anomalies over its southern center. Equatorial wave patterns suggested that eastern Pacific could be the main forcing region. This was also the area of the strongest wave activity. However, additional modeling studies are needed in order to confirm that propagation of Rossby wave trains into the North Atlantic due to forcing by the tropical Pacific heating is the actual mechanism for persistence of the positive phase of the decadal NAO.

To examine the local effect of the SSTs on the multi-year persistence of the NAO additional experiment with COLA AGCM was conducted where the anomalous SST forcing was limited only to the North Atlantic region. Although the model response in the North Atlantic displayed a dipole pattern characteristic of the positive phase of the NAO, both 500-hPa geopotential height and SLP anomalies were not strong enough to be statistically significant, except for the northern center in the 500-hPa geopotential height field which was somewhat stronger than in the 8895 TropIP experiment but was shifted much further to the west. Analysis of the North Atlantic variability in the model revealed the dominance of the NAO with very realistic spatial structure. Nevertheless, the mean of these coherent fluctuations was apparently too weak and the variance was too high to make them statistically different from the NAO fluctuations in the CLIM experiment. The largest statistically significant precipitation anomalies in this experiment were observed in the equatorial Atlantic and extreme eastern equatorial Pacific during months of July through November. In the equatorial Atlantic these anomalies were very similar to the ones from the 8895 GLOBAL simulation, whereas in the 8895 IPT experiment there were no significant anomalies present in this region. During late fall and winter

significant precipitation response was observed only in the equatorial Atlantic. Though statistically significant, it was weaker in magnitude and smaller in scale compared to the precipitation anomalies from the 8895 GLOBAL and 8895 TropIP experiments both in equatorial Pacific and Atlantic. Results from this experiment suggest that boundary forcing in the Atlantic confined primarily to the equatorial region is not strong enough to significantly affect the phase of the decadal NAO.

Acknowledgments

This study was performed as a partial fulfillment of the requirements for the degree of Doctor of Philosophy in Climate Dynamics at the School of Computational Sciences, George Mason University. I would like to express my sincere gratitude to Dr. Shukla for his patience, strong support and direction during my dissertation work and also throughout the years of studying at George Mason University. I would like to thank Larry Marx for his help with the COLA model. I would also like to thank Drs. Schopf, Straus, Kirtman and Schneider for their advice and many useful comments.

References

Hoerling, M. P., Hurrell, J. W., Xu, T. 2001 "Tropical origins for recent North Atlantic climate change", *Science*, **292**, 90-92

Huang, J., Higuchi, K., and Shabbar, A. 1998 "The relationship between the North Atlantic Osicllation and El Niño-Southern Oscillation", *Geophys. Res. Lett*., **25**, 2707-2710.

Hurrell J. W. 1995 "Decadal trends in the North Atlantic Oscillation: regional temperatures and precipitation", *Science*, **269**, 676-679.

Hurrell, J. W. and van Loon, H. 1997 "Decadal variations of climate associated with the North Atlantic Oscillation", *Climate Change*, **36**, 3101-326.

Grötzner, A., Latif, M., Dommenget, D. 2000 "Atmospheric response to sea surface temperature anomalies during El Nino 1997/98 as simulated by ECHAM4", *Quart. J. R. Met. Soc.,* **126**, 2175-2198.

Jin, F and Hoskins, B.J. 1995 "The Direct Response to Tropical Heating in a Baroclinic Atmosphere", *J. Atmos. Sci.*, **52**, 307-319.

Mehta, V. M., Suarez, M. J., Manganello, J. V. and Delworth, T. L. 2000 "Oceanic influence on the North Atlantic Oscillation and associated Northern Hemisphere climate variations: 1959-1993", *Geophys. Res. Letters*, **27**, 121-124.

Rodwell, M. J., Rowell, D. P. and Folland, C. K. 1999 "Oceanic forcing of the wintertime North Atlantic Oscillation and European climate", *Nature*, **398**, 320-323.

Roeckner, E., Kirchner, I., Oberhuber, J. M., Bacher, A., Christoph, M. 1996 "ENSO variability and atmospheric response in a global coupled atmosphere-ocean GCM", *Climate Dynamics*, **12**, 737-754.

Sardeshmukh, P.D., and Hoskins, B.J., 1988 "The generation of global rotational flow by steady idealized tropical divergence", *J. Atmos. Sci*., **45**, 1228-1251.

Schneider, E.K., 2002 "Understanding differences between the Equatorial Pacific as simulated by two coupled GCMs", *J. Climate*, **15**, 449-469.

Straus, D. M., Shukla, J. 2002 "Does ENSO force the PNA?", *J. Climate*, **15**, 2340-2358.

Von Storch, H. and Zwiers, F. W., 1999 "Statistical Analysis in Climate Research", Cambridge University Press, 484 pp.

Table 1. Averages and Standard Deviations of the NAO Indices. [1] NAO Index is defined as a difference of normalized DJFM SLP anomalies between stations at Ponta Delgada, Azores and Stykkisholmur, Iceland for the period of 1865-1997 and low-pass filtered with cut-off period at 6 years. [2] NAO Index is defined as a difference of normalized DJFM SLP anomalies from NCEP data averaged approximately over locations of Ponta Delgada, Azores and Stykkisholmur, Iceland for the period of 1949-1998 and low-pass filtered with cut-off period at 7 years. [3] NAO Index is defined as a difference of normalized DJFM SLP anomalies from the model data averaged approximately over locations of Ponta Delgada, Azores and Stykkisholmur, Iceland. [4] NAO Index is defined as a difference of normalized DJFM SLP anomalies from the model data averaged approximately over locations of Ponta Delgada, Azores and Stykkisholmur, Iceland. SLP climatology is taken from the CLIM experiment.

	Average	**Standard Deviation**
LPF≥6 Station NAO Index for 1865-1997[1]	1.76 over 1988-1995 -1.78 over 1961-1968	1.13
LPF≥7 NCEP NAO Index for 1949-1998[2]	1.80 over 1988-1995 -1.75 over 1961-1968	1.35
NAO Index from CLIM experiment using 50 years of data[3]	0	1.66
NAO Index from 8895 GLOBAL experiment using 50 years of data[4]	1.32	1.81
NAO Index from 8895 TropIP experiment using 50 years of data[4]	1.21	1.62
NAO Index from 8895 Natl experiment using 50 years of data[4]	0.66	1.78

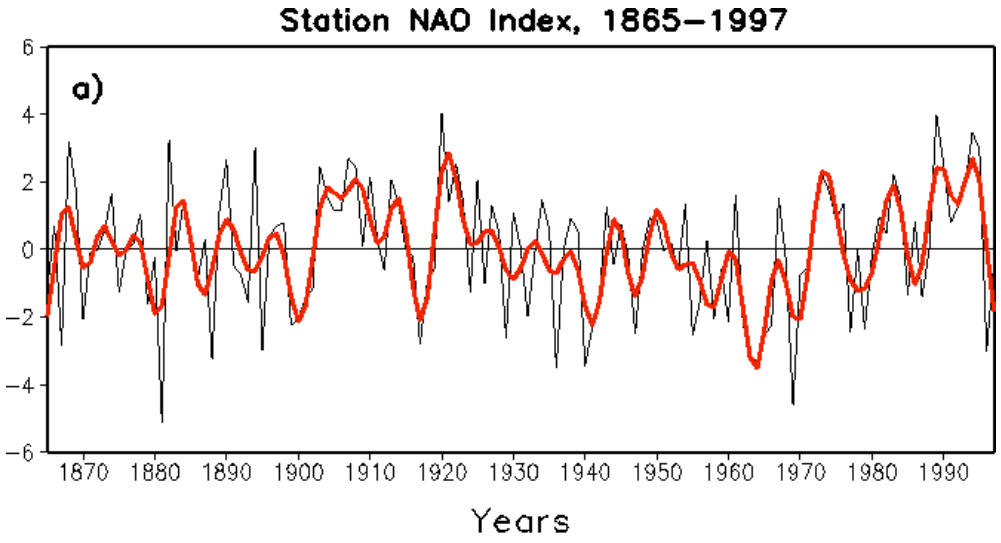

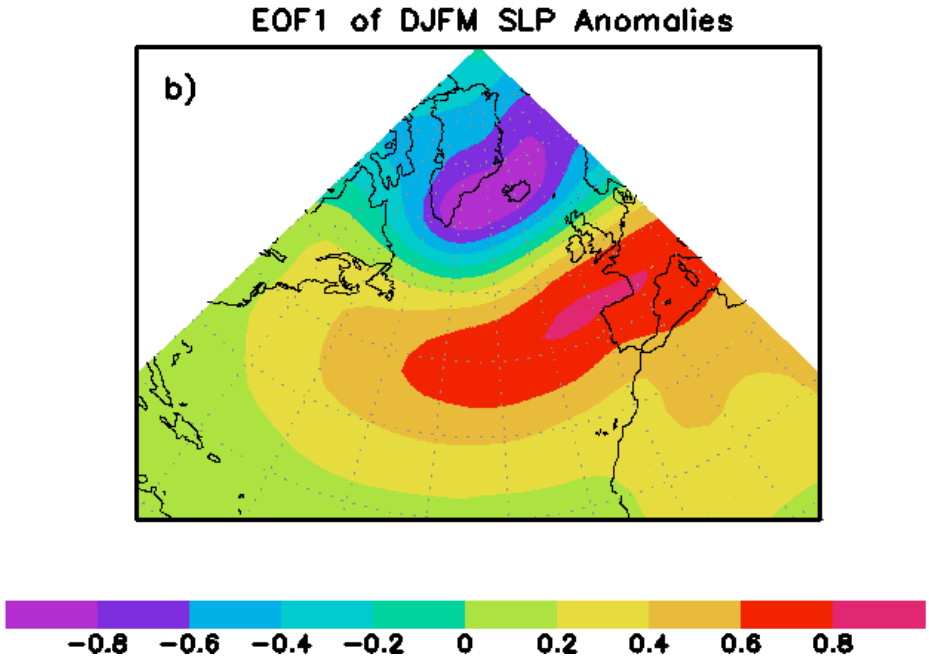

Figure 1. a) Time series of the Station NAO Index defined as a difference of normalized December-March average SLP anomalies between Ponta Delgada, Azores, and Stykkisholmur, Iceland from 1865 to 1997. The heavy red line represents the Station NAO Index time series smoothed with the low pass filter to remove fluctuations with periods less than 5 years; b) the leading North Atlantic EOF of DJFM average SLP anomalies from NCEP data for 1949-1998. The EOF is computed over the region 0-90ºN, 80ºW-12.5ºE. Map is from 20ºN -90ºN, 80ºW-12.5ºE.

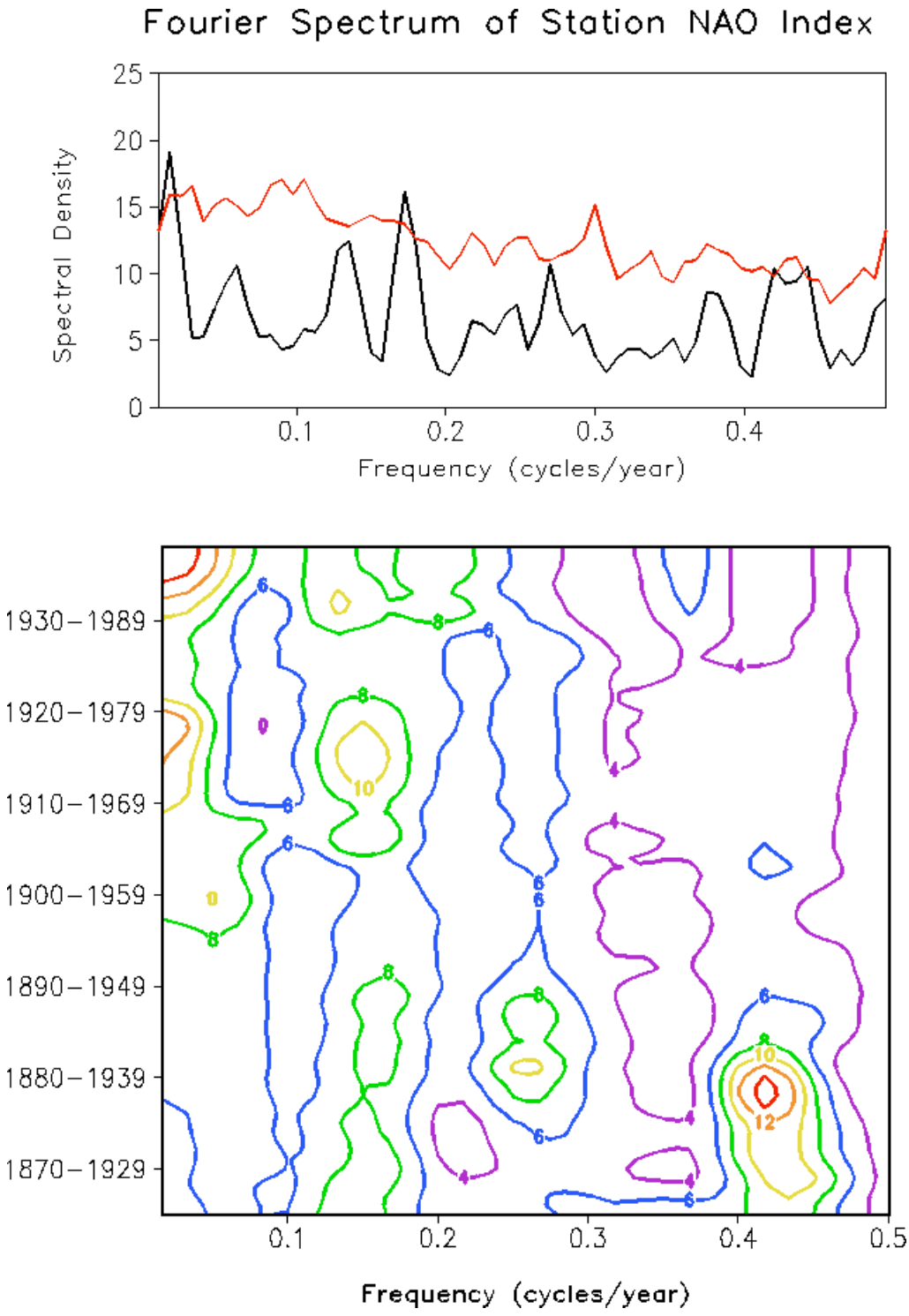

Figure 2. Power spectra of the Station NAO Index for 1865-1997 (top) and smoothed power spectra of running 60-year intervals of the Station NAO Index (bottom). Red line represents 90% confidence limit (top).

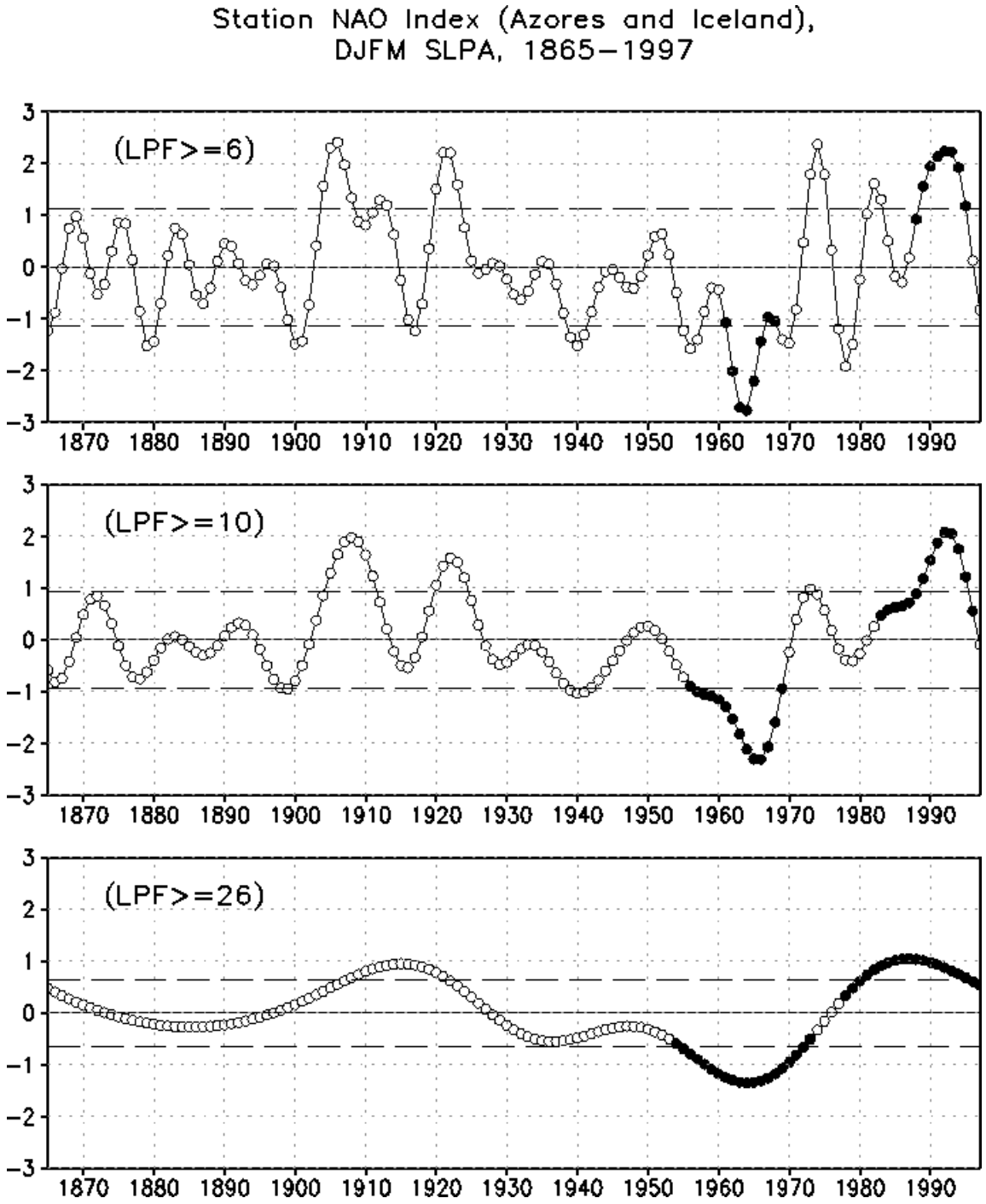

Figure 3. NAO Index (see definition in the text) for the period of 1865-1997 low-pass filtered with cut-off periods at 6 years (top panel), 10 years (middle panel) and 26 years (bottom panel). Dashed lines show the values of average plus (minus) standard deviation of the respective LPF NAO Index time series. Solid lines represent the average of each time series. Filled circles designate the periods of strong positive and negative NAO persistence according to the definition in the text.

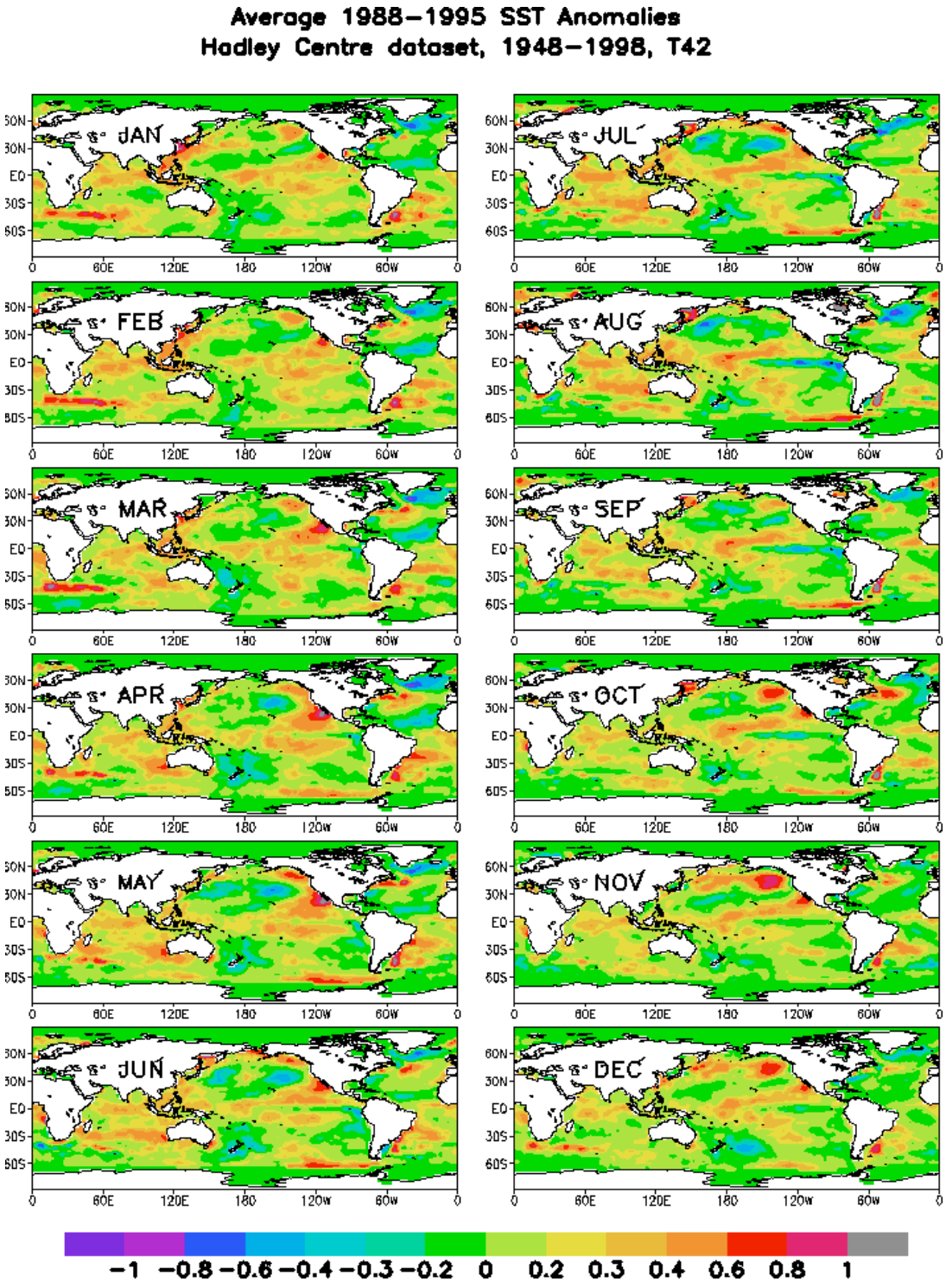

Figure 4. Annual cycle of the global SST anomalies from Hadley Centre dataset averaged over 1988-1995 corresponding to the period of strong persistence of the positive phase of the NAO based on the LPF ≥ 6 NAO Index.

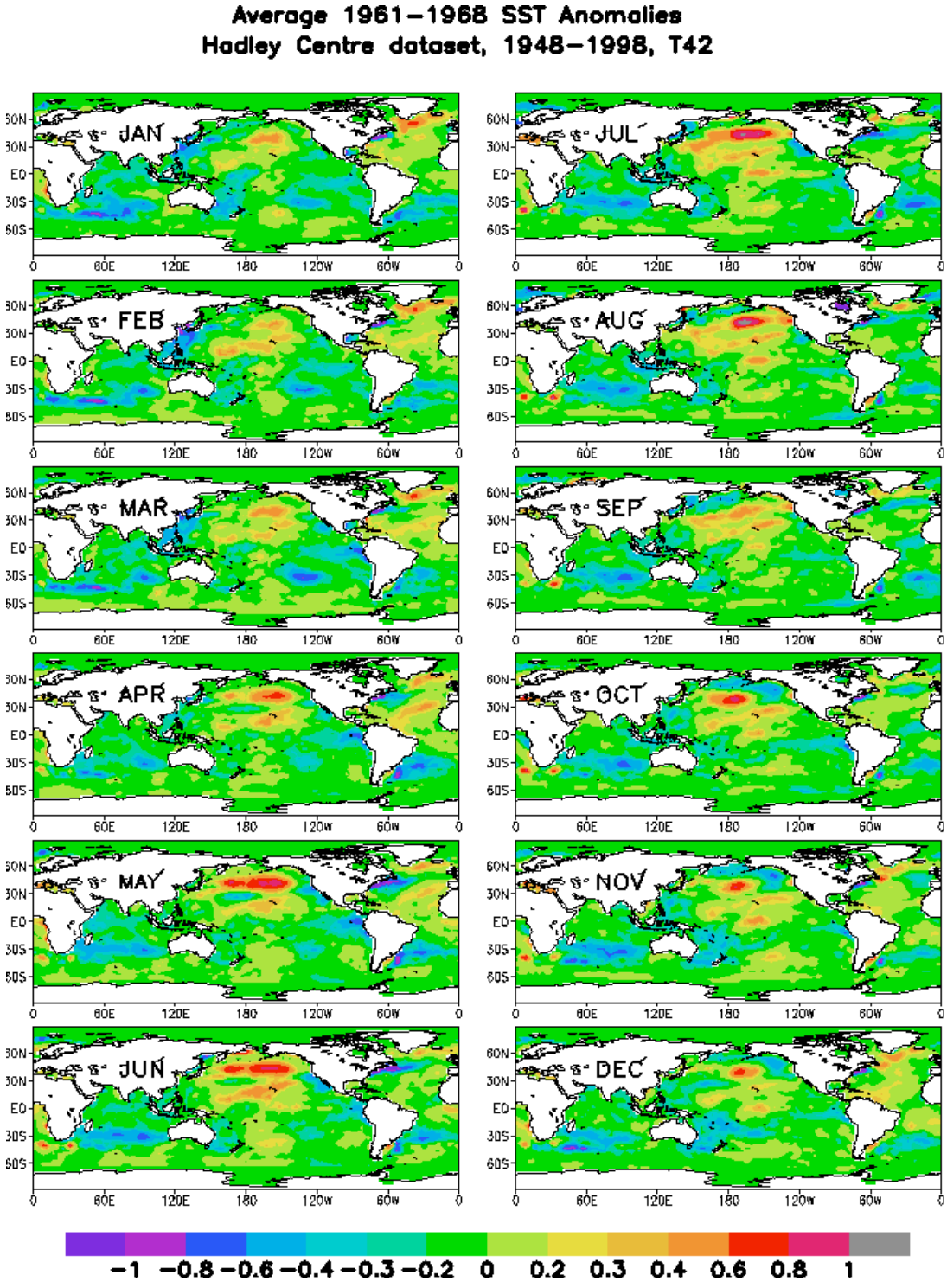

Figure 5. Annual cycle of the global SST anomalies from Hadley Centre dataset averaged over 1961-1968 corresponding to the period of strong persistence of the negative phase of the NAO based on the LPF ≥ 6 NAO Index.

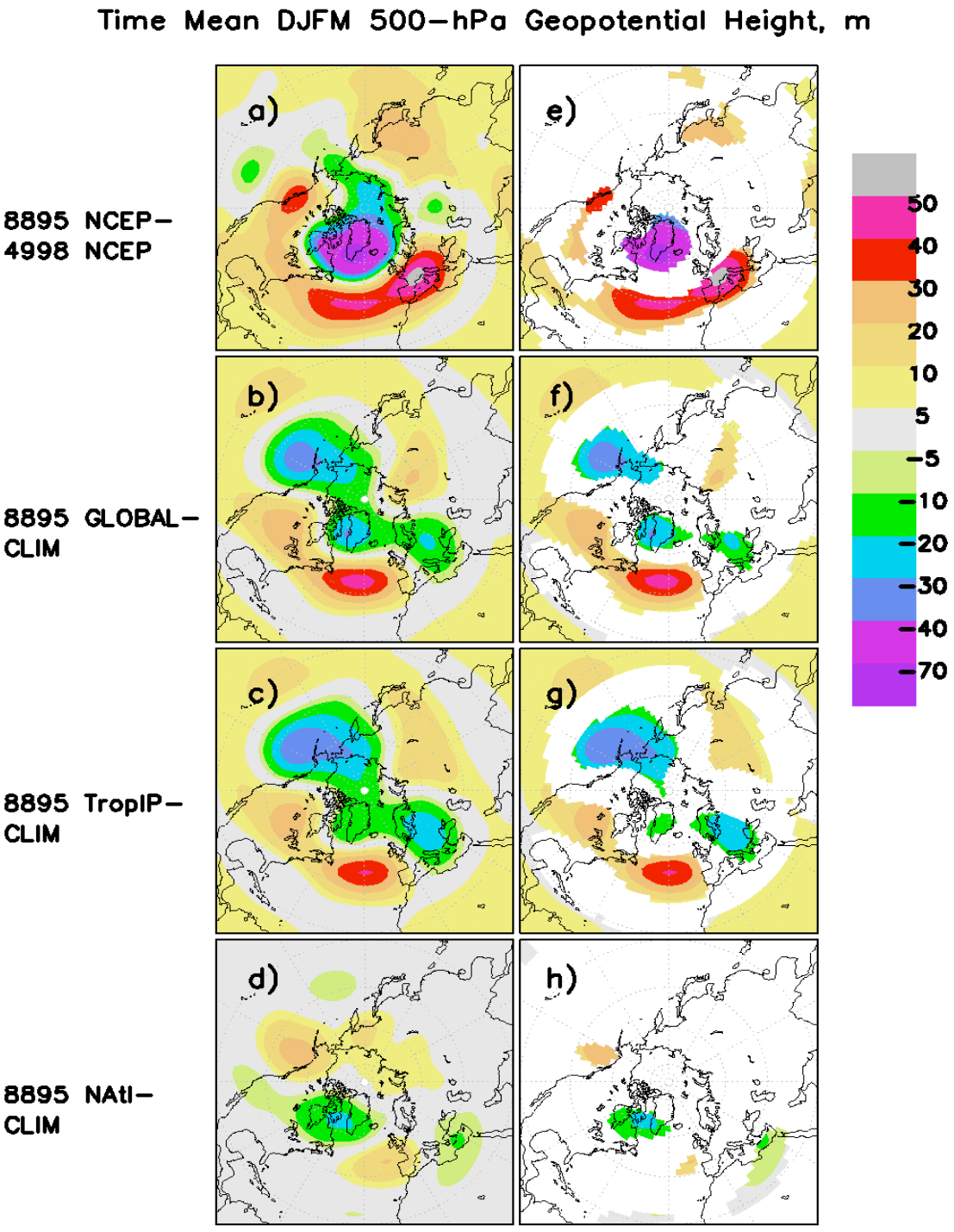

Figure 6. DJFM 500-hPa Geopotential Height a) from NCEP reanalysis averaged over 1988-1995 compared to the 1949-1998 average; averaged over 50 years of model integration from b) 8895 GLOBAL experiment compared to CLIM experiment, c) 8895 TropIP experiment compared to CLIM experiment, d) 8895 NAtl experiment compared to CLIM experiment. Units are m. Maps are of the Northern Hemisphere north of 20°N. e), f), g), h) are same as a), b), c) and d), except only grid points that are significant at 95% confidence level according to the pointwise Student's *t*-test are shown.

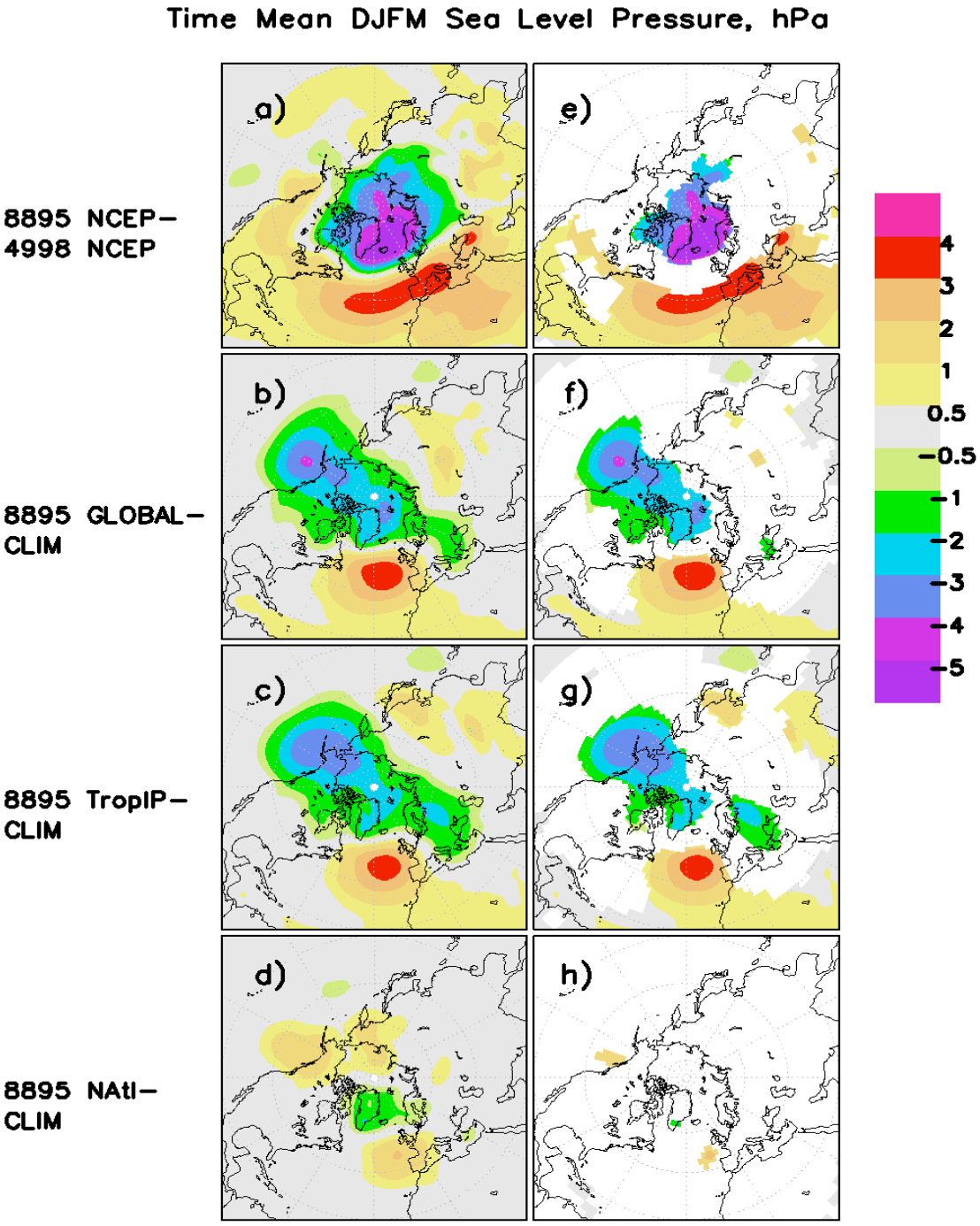

Figure 7. DJFM Sea Level Pressure a) from NCEP reanalysis averaged over 1988-1995 compared to the 1949-1998 average; averaged over 50 years of model integration from b) 8895 GLOBAL experiment compared to CLIM experiment, c) 8895 TropIP experiment compared to CLIM experiment, d) 8895 NAtl experiment compared to CLIM experiment. Units are hPa. Maps are of the Northern Hemisphere north of 20°N. E), f), g), h) are same as a), b), c) and d), except only grid points that are significant at 95% confidence level according to the pointwise Student's *t*-test are shown.

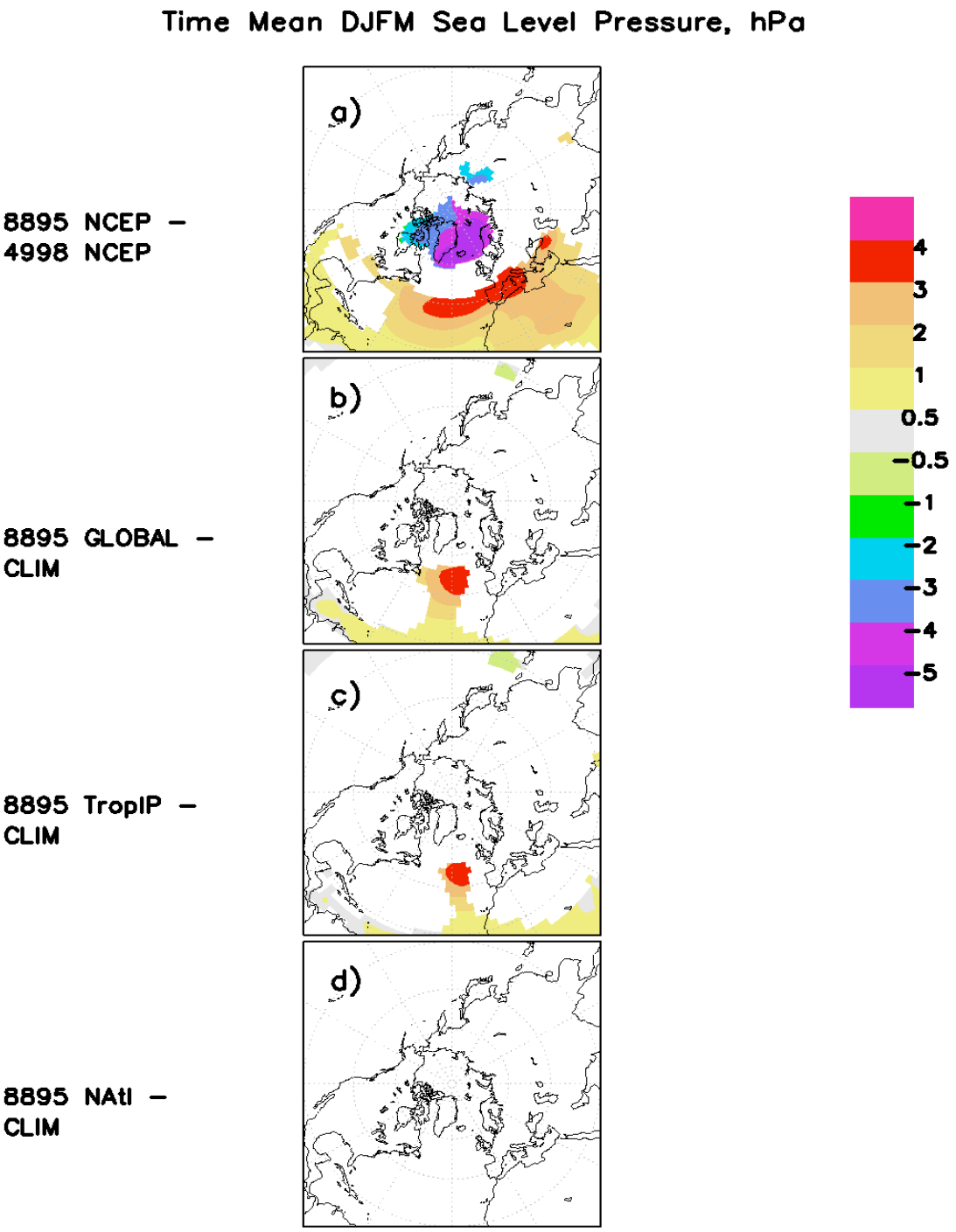

Figure 8. DJFM Sea Level Pressure a) from NCEP reanalysis averaged over 1988-1995 compared to the 1949-1998 average; averaged over 50 years of model integration from b) 8895 GLOBAL experiment compared to CLIM experiment, c) 8895 TropIP experiment compared to CLIM experiment, d) 8895 NAtl experiment compared to CLIM experiment. Units are hPa. Maps are of the Northern Hemisphere north of 20°N. Only grid points at which the pointwise estimate of (0.5,p)-recurrence is less than 20% or greater than 80% are shown.

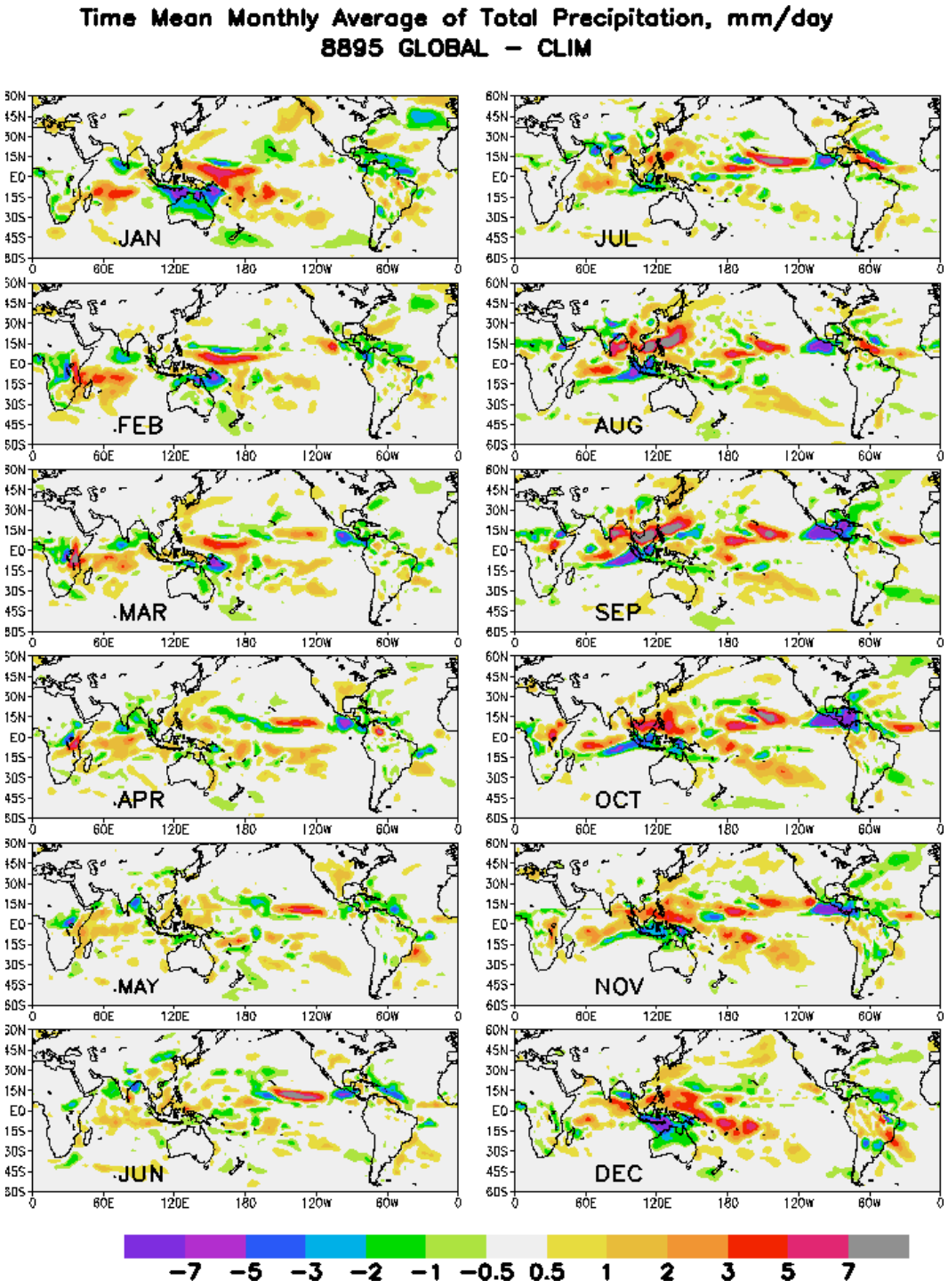

Figure 9. Difference of time mean monthly average of total precipitation from the 8895 GLOBAL experiment and the CLIM experiment. Fifty years of model integration are used to calculate time mean monthly averages. Units are mm/day. All maps are from 60° S to 60° N.

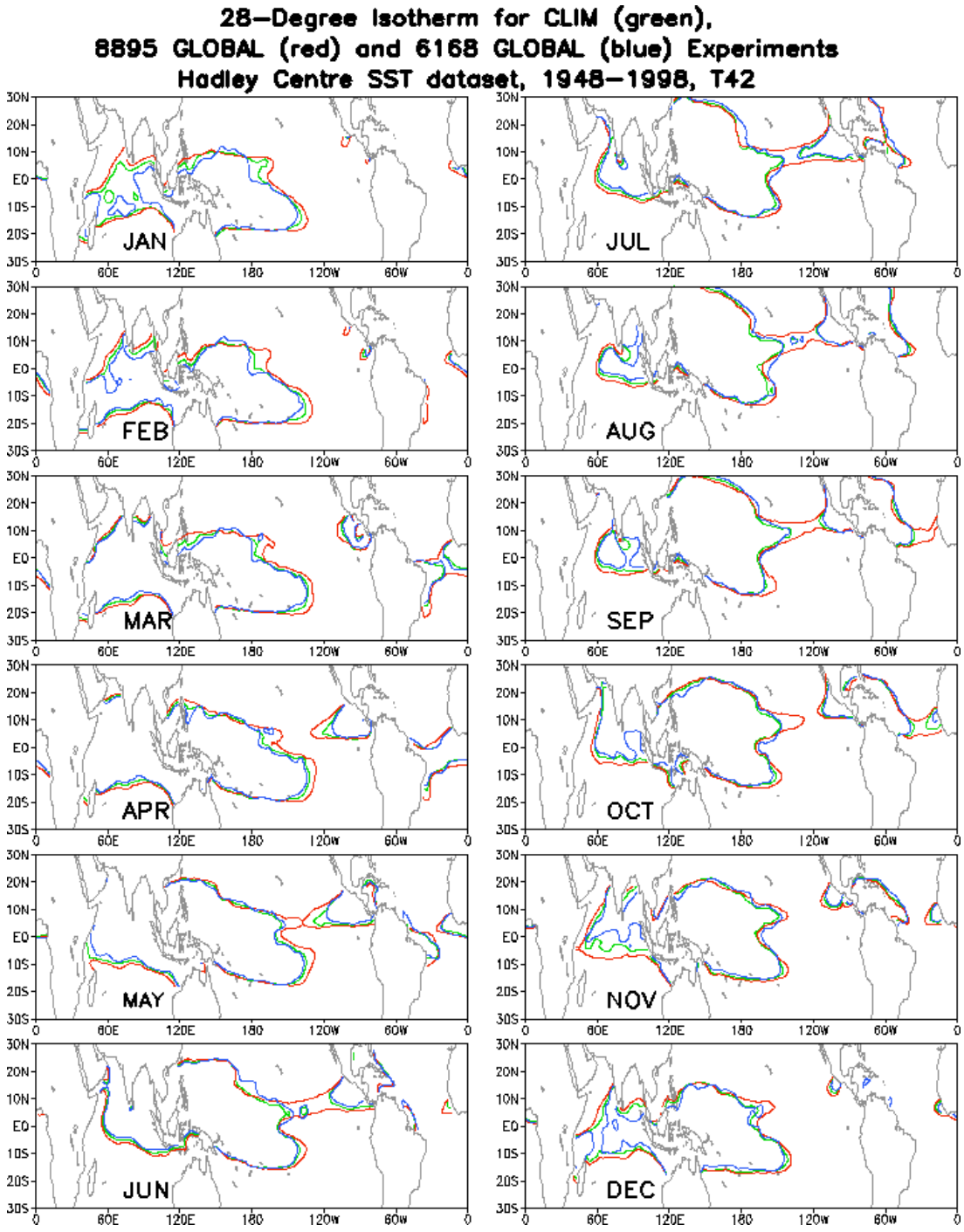

Figure 10. Annual cycle of the 28-degree isotherm in the SST distribution used to force CLIM experiment (green contours), 8895 GLOBAL experiment (red contours) and 6168 GLOBAL experiment (blue contours). Hadley Centre SST data from 1948-1998 is used to calculate SST climatology and average SST anomalies during 1988-1995 and 1961-1968. All maps are from 30° S to 30° N.

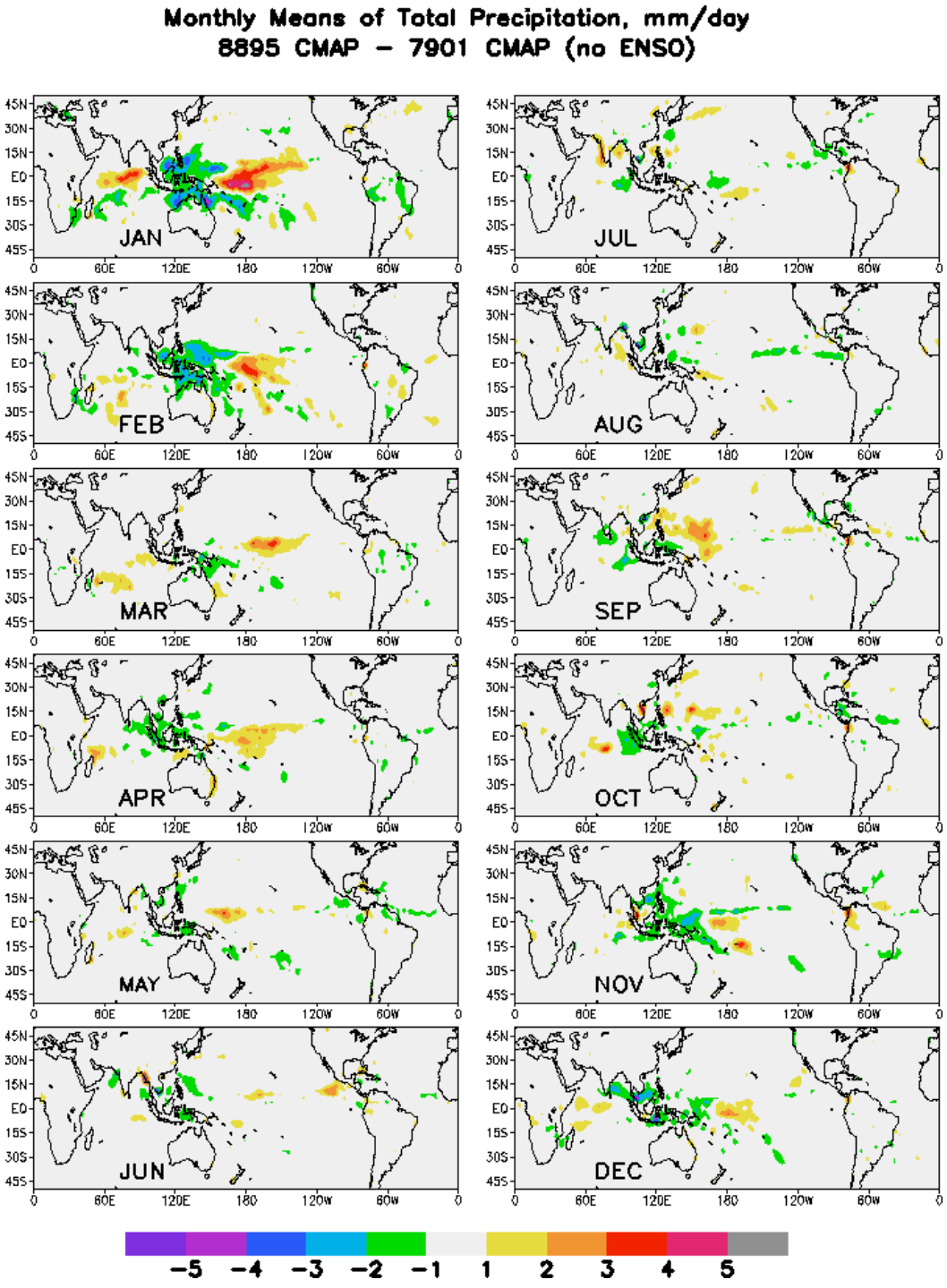

Figure 11. Difference of monthly means of total precipitation averaged over 1988-1995 and 1979-2001 where strong ENSO years were excluded from the 1979-2001 averaging period (see text for details). CMAP data of Xie and Arkin. Units are mm/day. All maps are from 50° S to 50° N.

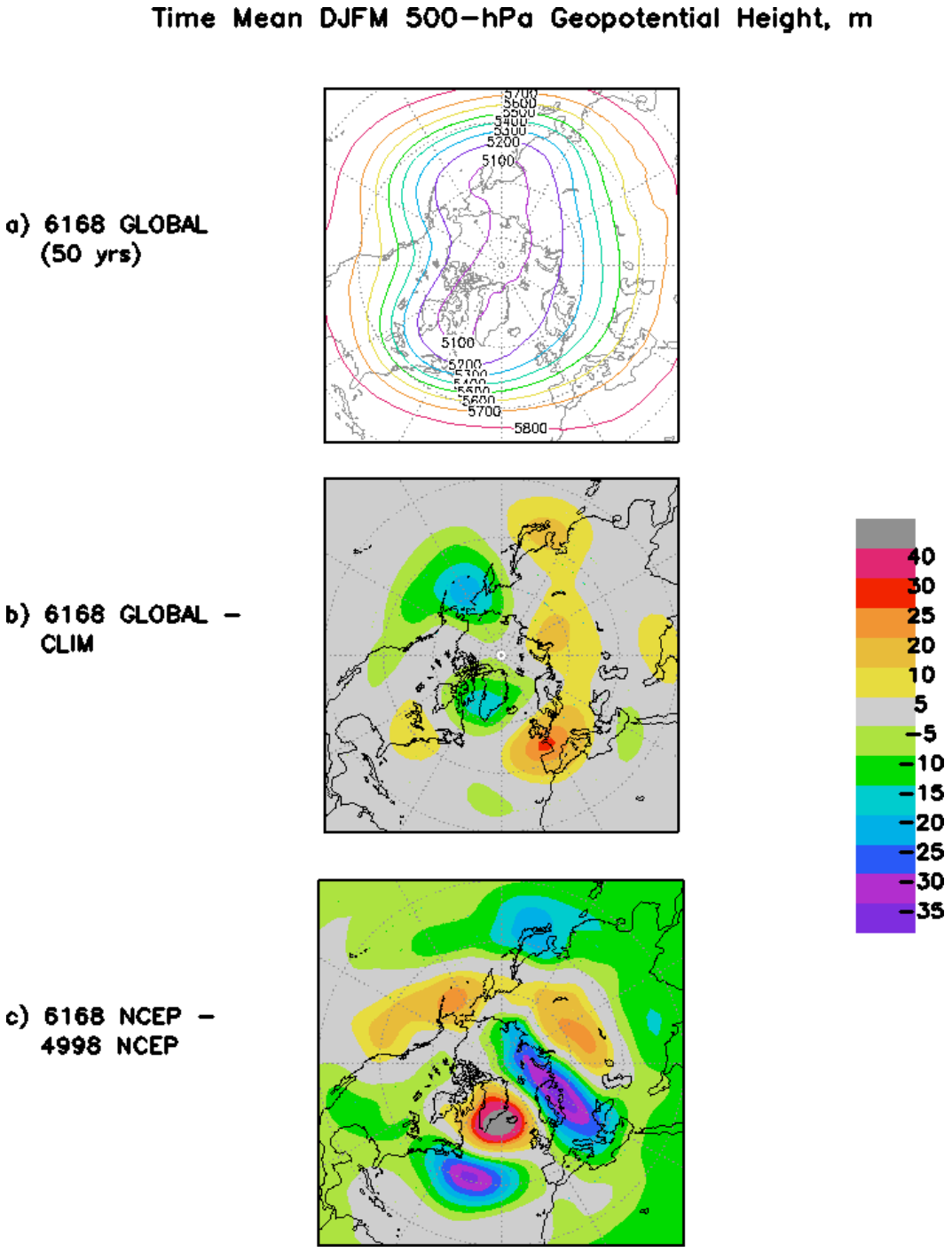

Figure 12. Time Mean DJFM 500-hPa geopotential height from a) 6168 GLOBAL experiment using 50 years of model integration, b) difference between 6168 GLOBAL and CLIM experiments, c) difference between NCEP data averaged over 1961-1968 and 1949-1998. Units are m. Contour interval is a) 100 m. Maps are of the Northern Hemisphere, north of 30°N in a), and north of 20°N in b) and c).

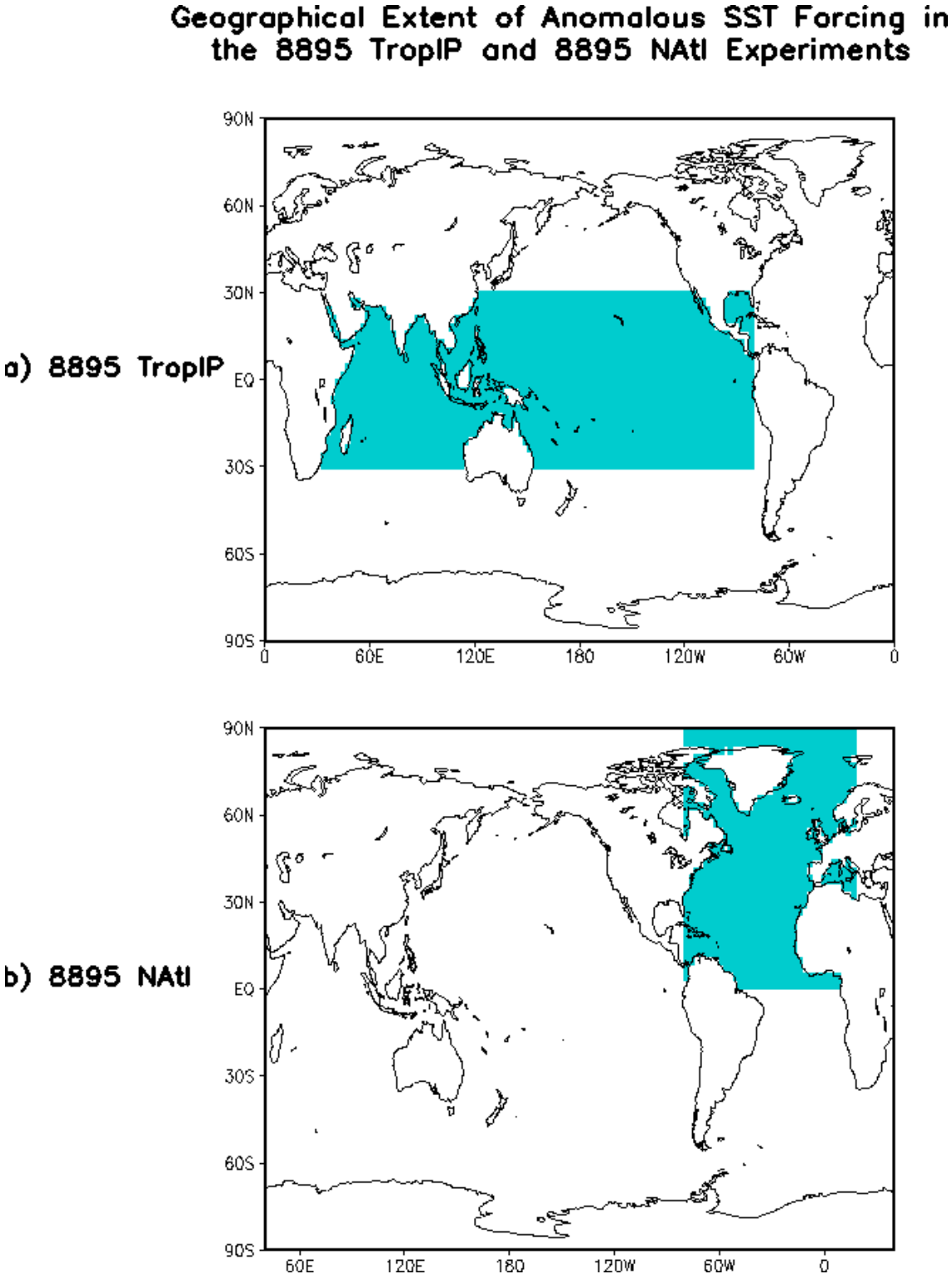

Figure 13. Shading indicates geographical extent of SST anomalies used in the a) 8895 TropIP experiment, b) 8895 NAtl experiment.

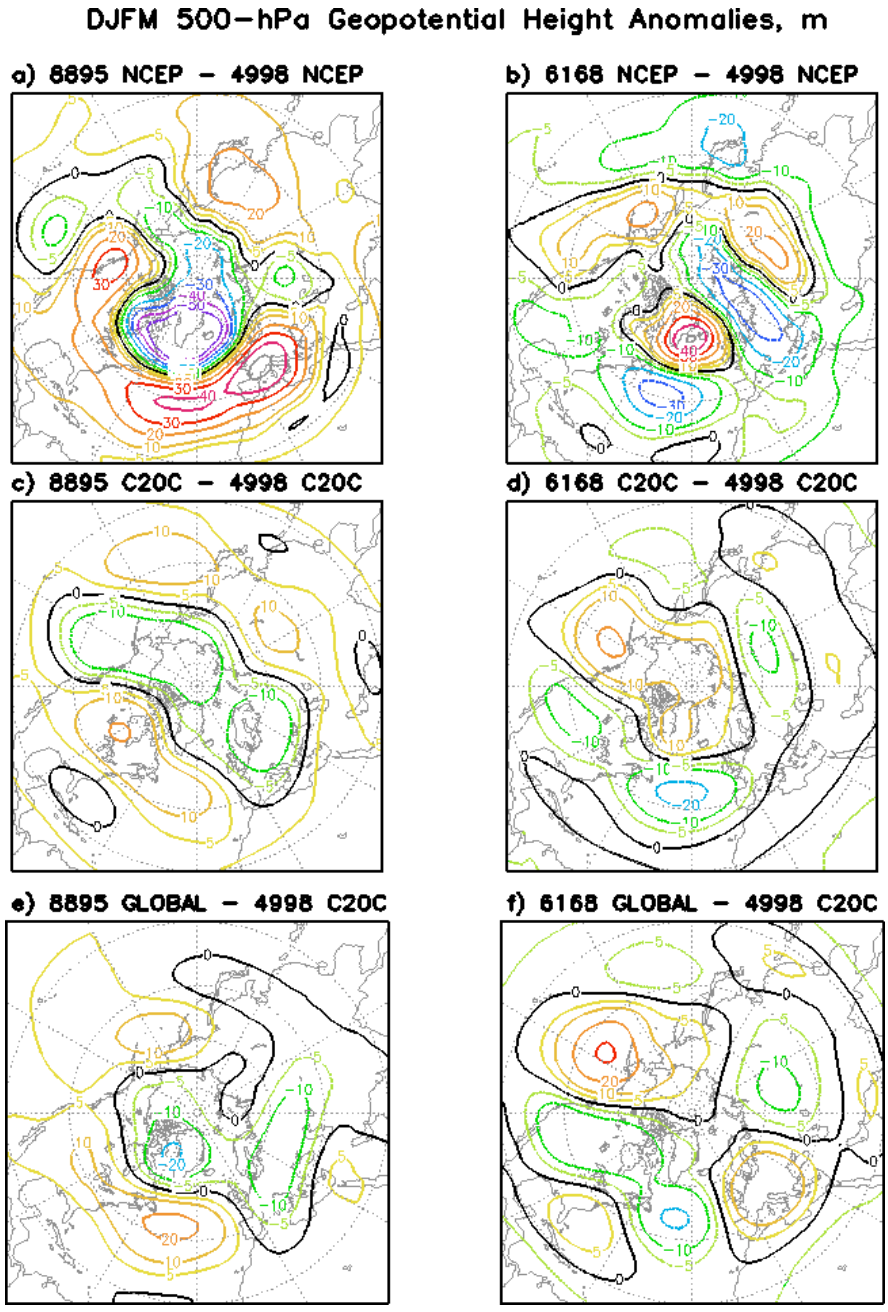

Figure 14. DJFM 500-hPa geopotential height anomalies from NCEP data averaged over a) 1988-1995, b) 1961-1968, both computed relative to NCEP 1949-1998 climatology; from C20C experiment data, ensemble-average and c) 1988-1995 average, d) 1961-1968 average, both computed with respect to ensemble-average 1949-1998 mean; from e) 8895 GLOBAL, f) 6168 GLOBAL experiment data averaged over 50 years of simulation, both computed with respect to C20C ensemble-average 1949-1998 mean. Units are m. Positive contours are solid, negative contours are dashed. Maps are of the Northern Hemisphere north of 20°N.

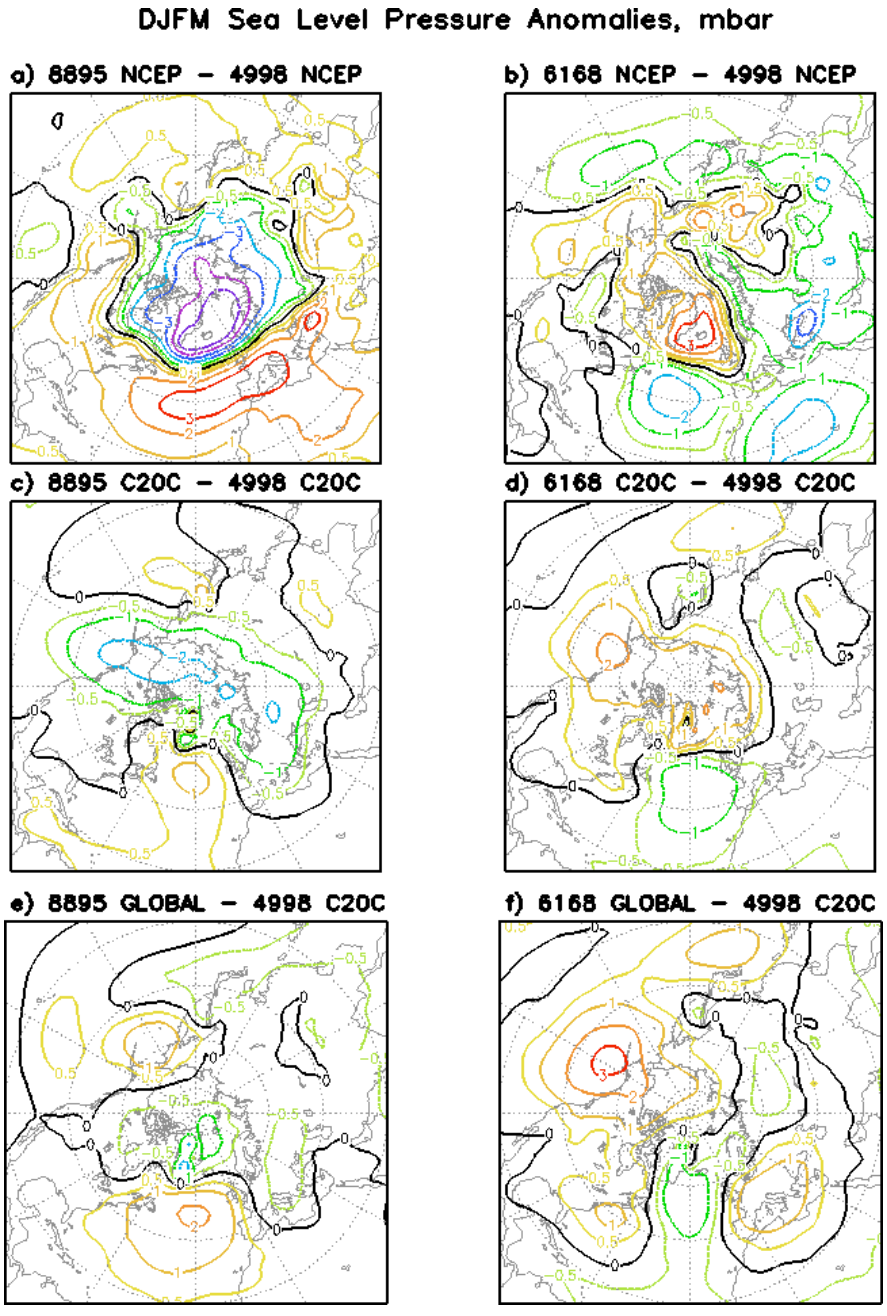

Figure 15. DJFM Sea Level Pressure anomalies from NCEP data averaged over a) 1988-1995, b) 1961-1968, both computed relative to NCEP 1949-1998 climatology; from C20C experiment data, ensemble-average and c) 1988-1995 average, d) 1961-1968 average, both computed with respect to ensemble-average 1949-1998 mean; from e) 8895 GLOBAL, f) 6168 GLOBAL experiment data averaged over 50 years of simulation, both computed with respect to C20C ensemble-average 1949-1998 mean. Units are mbar. Positive contours are solid, negative contours are dashed. Maps are of the Northern Hemisphere north of 20°N.

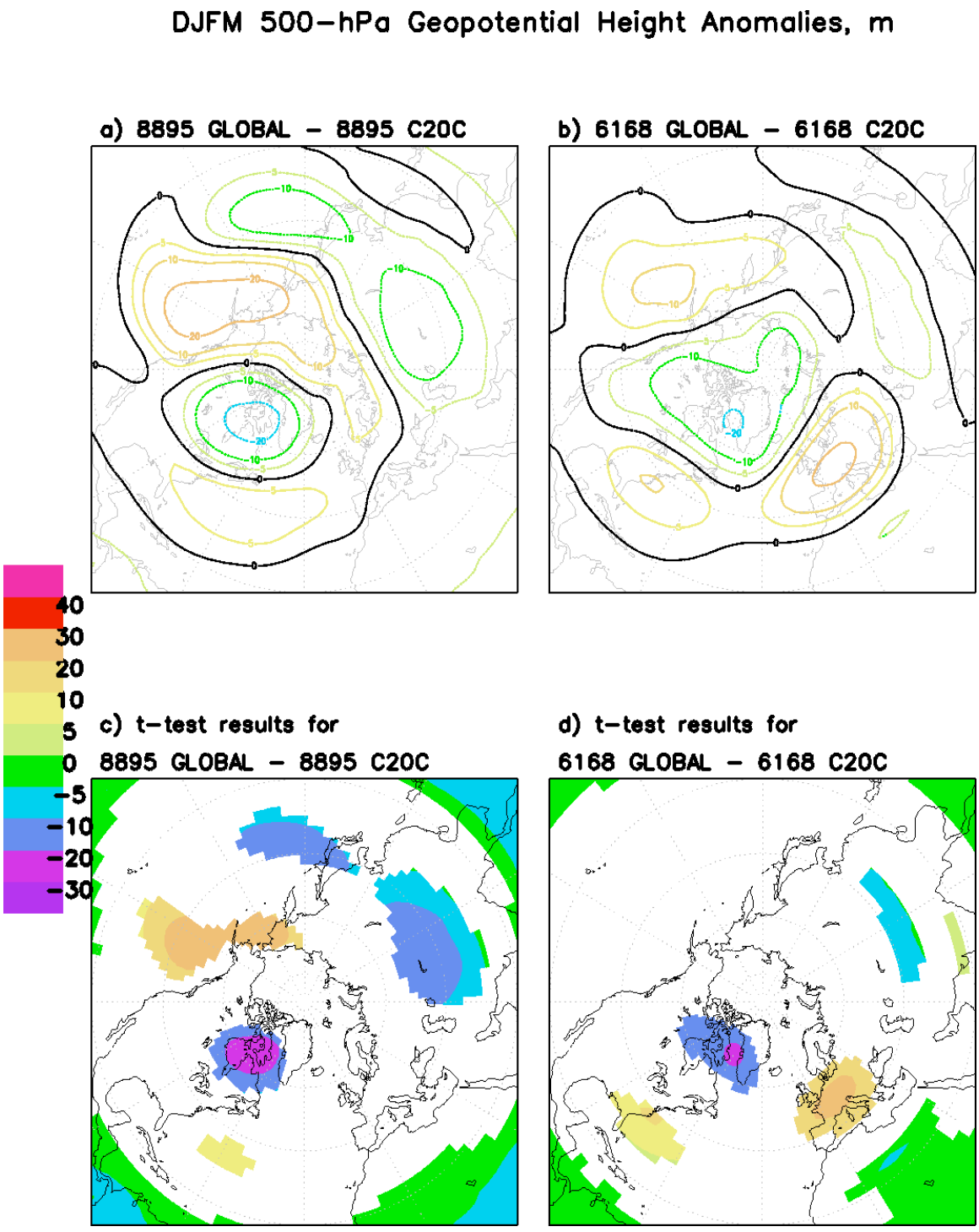

Figure 16. Difference of DJFM 500-hPa geopotential height response from a) 8895 GLOBAL experiment data and ensemble-average, 1988-1995 average C20C experiment data; b) 6168 GLOBAL experiment data and ensemble-average, 1961-1968 average C20C experiment data; c) and d) are the same as a) and b) except that only grid points that are significant at 95% confidence level according to the pointwise Student's *t*-test are shown. Units are m. Maps are of the Northern Hemisphere north of 20°N.

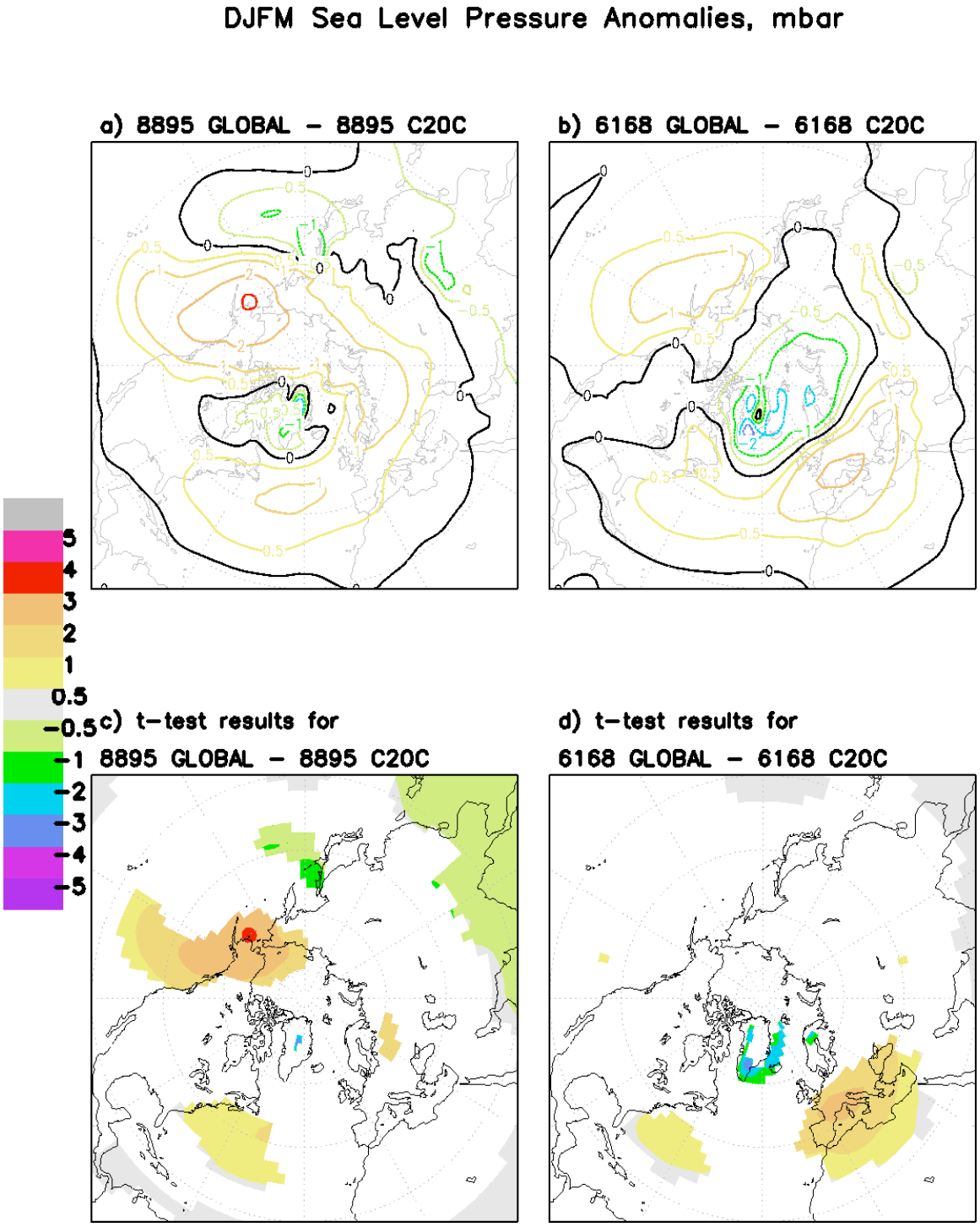

Figure 17. Difference of DJFM Sea Level Pressure response from a) 8895 GLOBAL experiment data and ensemble-average, 1988-1995 average C20C experiment data; b) 6168 GLOBAL experiment data and ensemble-average, 1961-1968 average C20C experiment data; c) and d) are the same as a) and b) except that only grid points that are significant at 95% confidence level according to the pointwise Student's *t*-test are shown. Units are mbar. Maps are of the Northern Hemisphere north of 20°N.

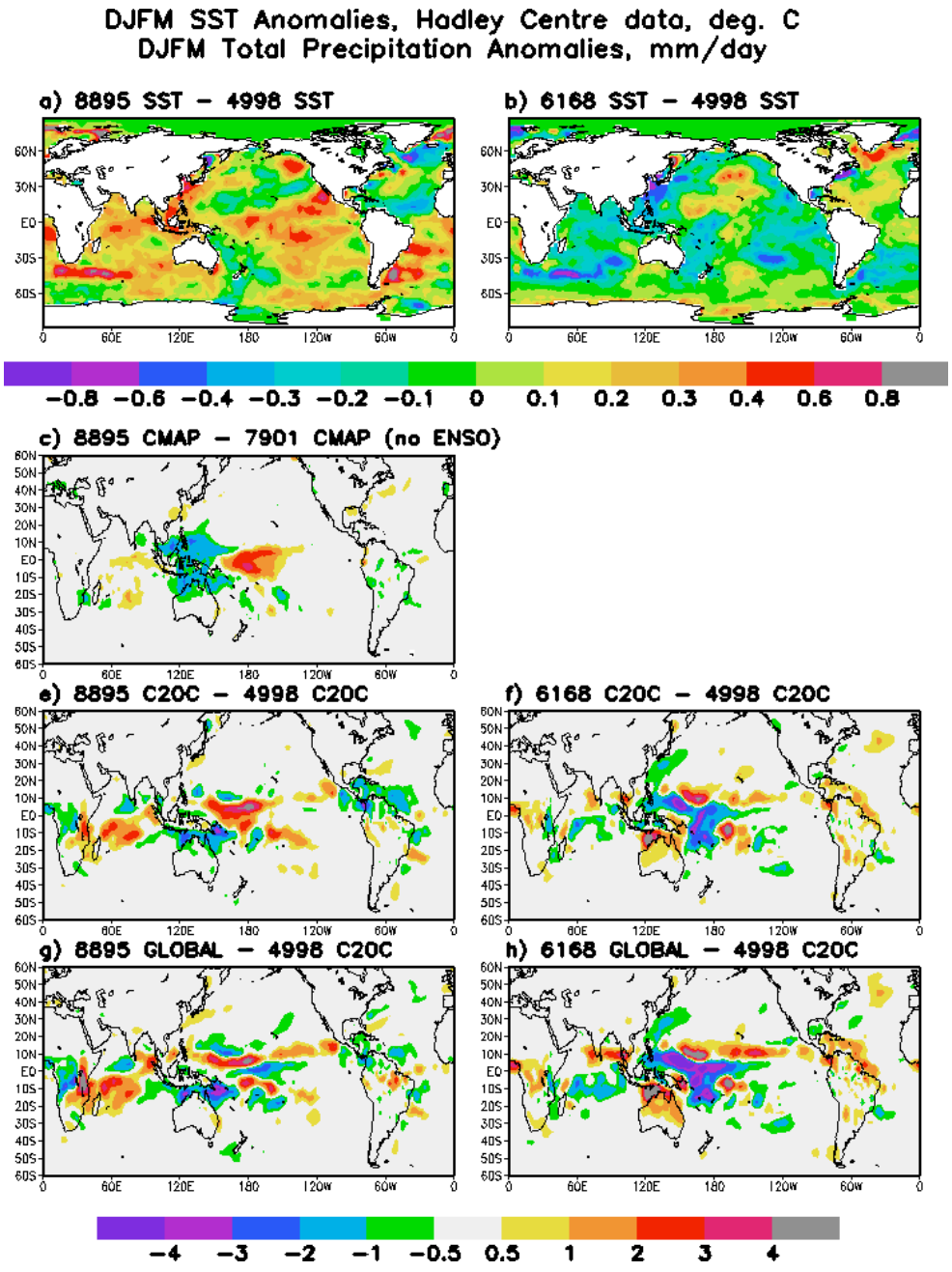

Figure 18. DJFM SST anomalies averaged over a) 1988-1995, b) 1961-1968, relative to the 1949-1998 climatology; DJFM total precipitation anomalies from c) CMAP data of Xie and Arkin, averaged over 1988-1995, relative to the 1979-2001 mean with ENSO years excluded; from ensemble-average C20C experiment data averaged over e) 1988-1995, f) 1961-1968, computed relative to the ensemble-average 1949-1998 mean; from g) 8895 GLOBAL, h) 6168 GLOBAL experiment data averaged over 50 years of simulation, computed with respect to the C20C ensemble-average 1949-1998 mean. Maps are global for a) and b), and 60°S to 60°N for c), e), f), g) and h).

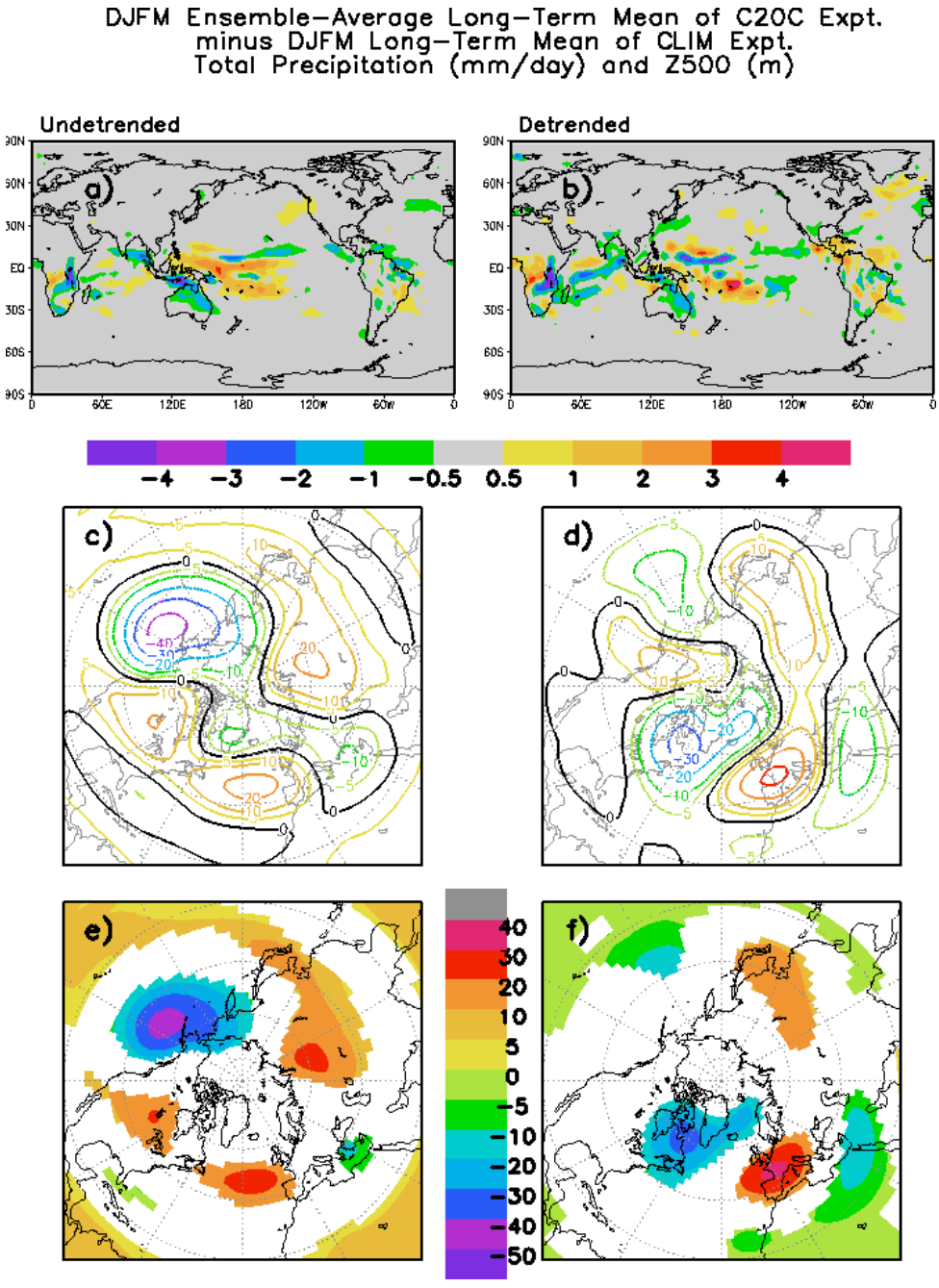

Figure 19. Difference of DJFM ensemble-average long-term mean of a) total precipitation, c) 500-hPa geopotential height from C20C data and DJFM long-term mean from CLIM experiment. Figs. b) and d) are the same as a) and c) except data is detrended. Figs. e) and f) are the same as c) and d) except only grid points that are significant at 95% confidence level according to the pointwise Student's t-test are shown. Units are mm/day for Figs. a) and b) and m for c), d), e) and f). Maps are global for Figs. a) and b) and of the Northern Hemisphere north of 20°N for c), d), e) and f).

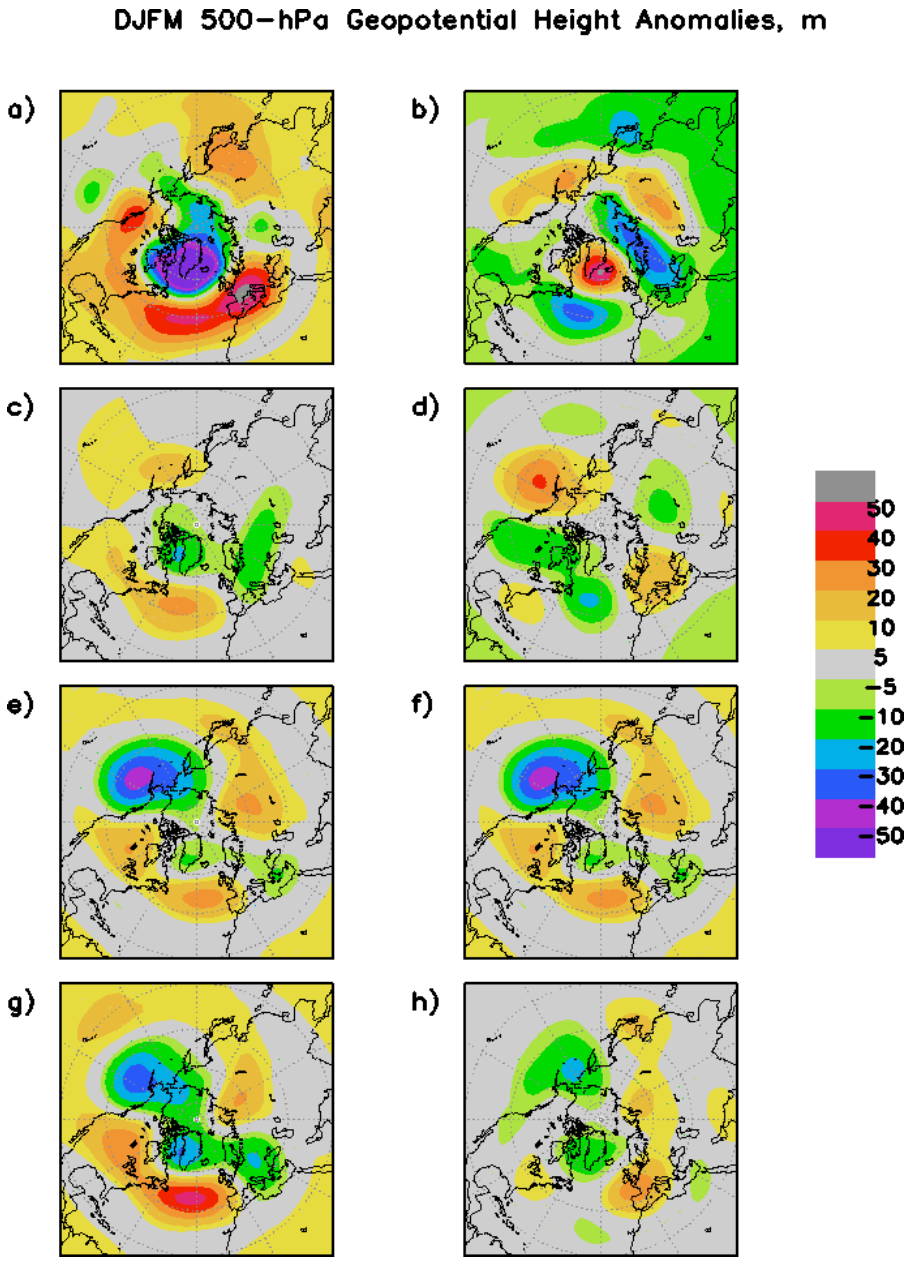

Figure 20. DJFM 500-hPa geopotential height anomalies from NCEP data averaged over a) 1988-1995, b) 1961-1968, computed relative to NCEP 1949-1998 climatology; from c) 8895 GLOBAL, d) 6168 GLOBAL experiment data averaged over 50 years of simulation, computed with respect to C20C ensemble-average 1949-1998 mean; from g) 8895 GLOBAL, h) 6168 GLOBAL experiment data averaged over 50 years of simulation, computed with respect to the long-term mean of CLIM experiment. e) Difference of DJFM ensemble-average long-term mean from C20C data and DJFM long-

term mean from CLIM experiment; f) is the same as e). Units are m. All maps are of the Northern Hemisphere north of 20°N.

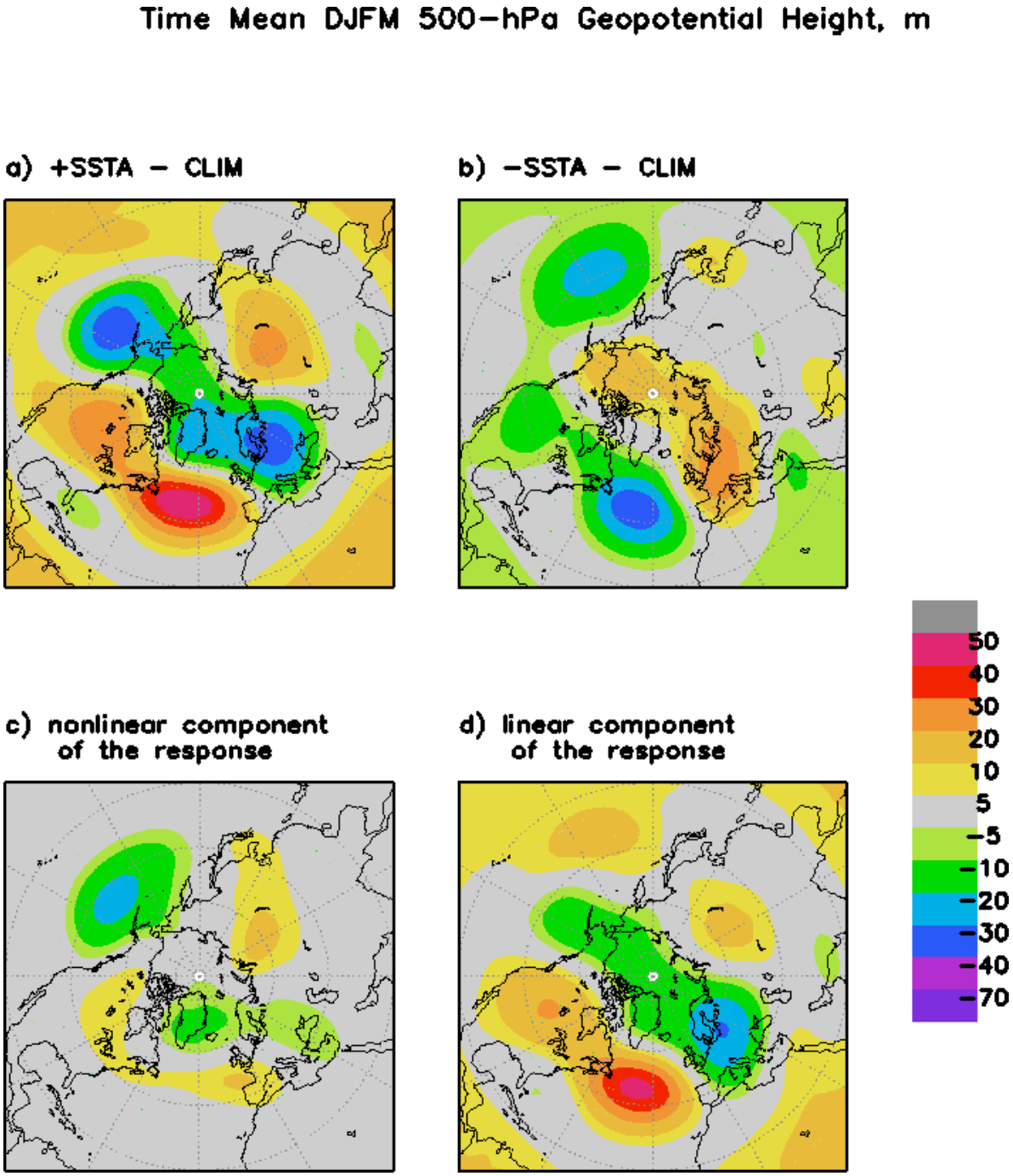

Figure 21. DJFM 500-hPa geopotential height averaged over 50 years of model integration from a) +SSTA experiment compared to CLIM experiment, b) -SSTA experiment compared to CLIM experiment; also shown c) non-linear and d) linear components of the forced response. Units are m. Maps are of the Northern Hemisphere north of 20°N.

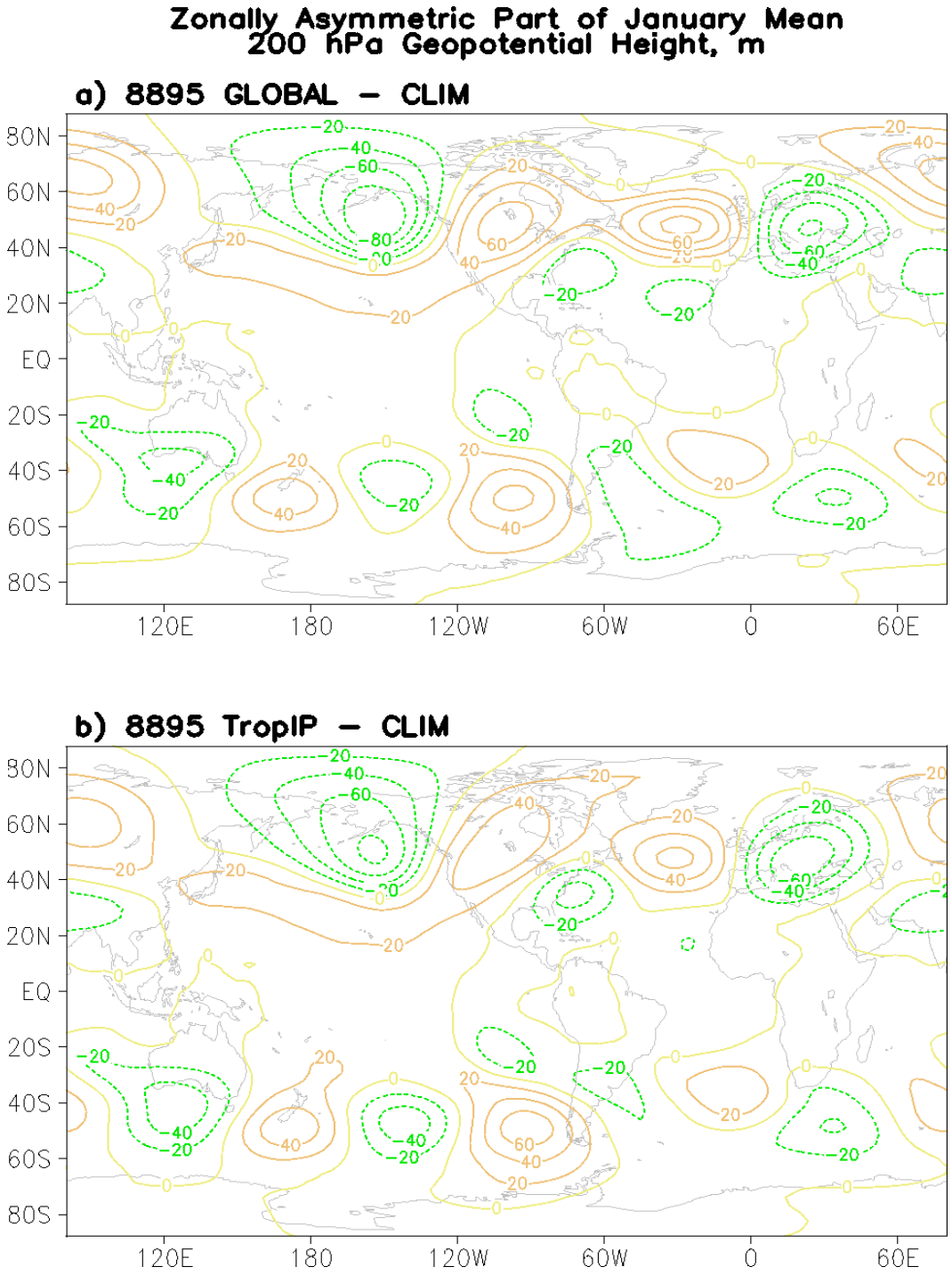

Figure 22. Zonally asymmetric part of January mean 200-hPa geopotential height from a) 8895 GLOBAL experiment compared to CLIM experiment, b) 8895 TropIP experiment compared to CLIM experiment. 50 years of model integration are used to calculate January means. Units are m. Contour interval is 20 m. Positive contours are orange with starting value of 20 m. Negative contours are green with starting value of –20 m. Zero contour is yellow. All maps are from 90° S to 90° N.

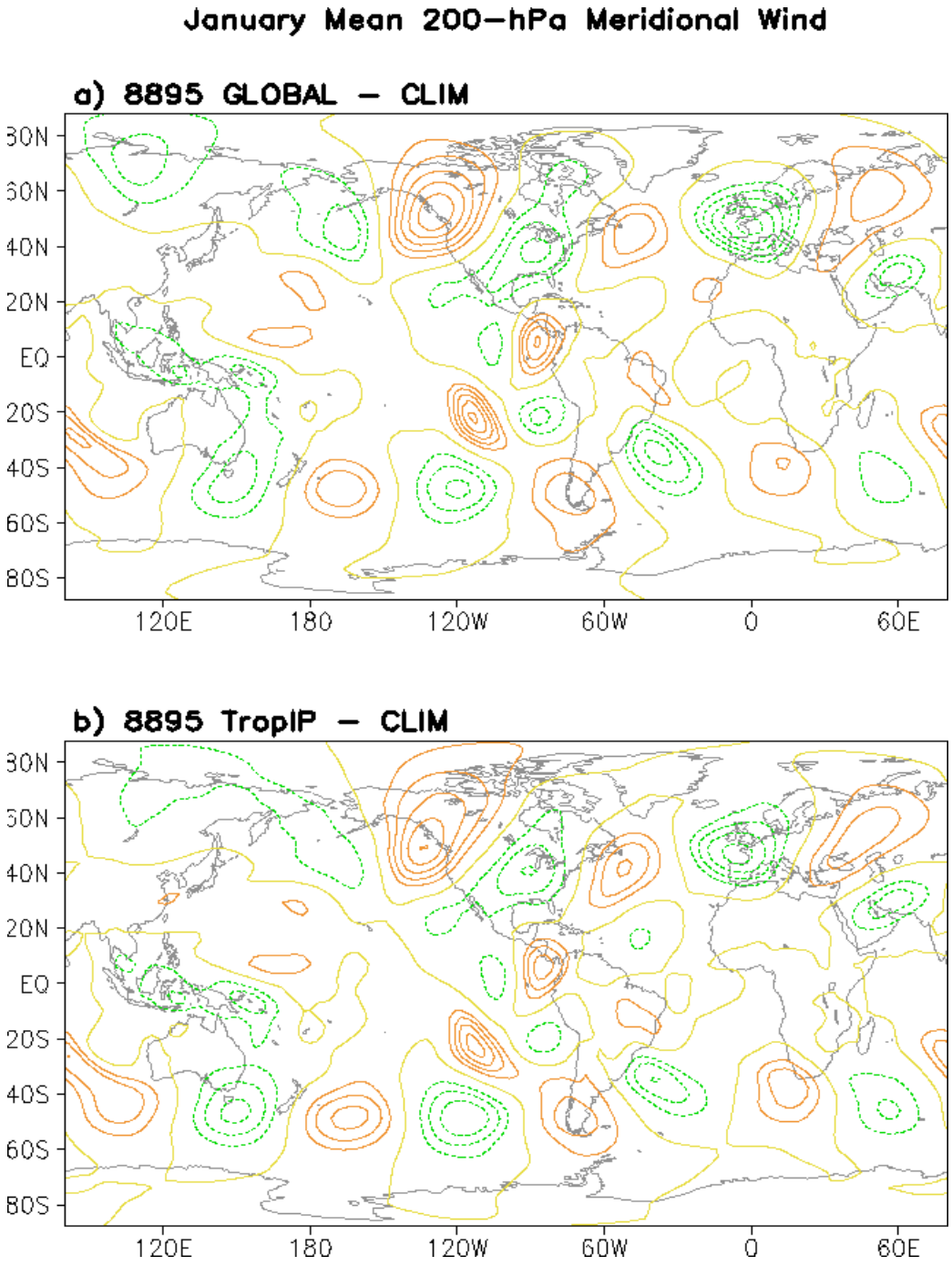

Figure 23. January mean 200-hPa meridional wind from a) 8895 GLOBAL experiment compared to CLIM experiment, b) 8895 TropIP experiment compared to CLIM experiment. 50 years of model integration are used to calculate January means. Units are m/s. Contour interval is 1m/s. Positive contours are orange with starting value of 2 m/s. Negative contours are green with starting value of –2 m/s. Zero contour is yellow. All maps are from 90° S to 90° N.